Dissertation

On

ANALYSIS AND REDESIGN OF A PORTABLE STAND

Submitted in partial fulfillment of the requirement

for the award of the degree of

Master of Engineering

in

CAD CAM

Submitted By

NAVDEEP KUMAR

Roll No. 851381002

Under the Guidance of

Mr. A. S. JAWANDA

Associate Professor

Department of Mechanical Engineering

Thapar Institute of Engineering &

Technology Patiala

THAPAR INSTITUTE
OF ENGINEERING & TECHNOLOGY
(Deemed to be University)

DEPARTMENT OF MECHANICAL ENGINEERING
THAPAR INSTITUTE OF ENGINEERING & TECHNOLOGY
PATIALA-147004, INDIA,

JULY – 2018

Dedication

I would like to dedicate this thesis to my family: My father and mother, Karam Chand and Chanchla Devi and my brother Dinesh Kumar.

Their unfailing support and continuous words of encouragement throughout these years will always be remembered…

DECLARATION

I hereby declare that the thesis entitled **"Analysis and Redesign of a Portable Stand"** is an authentic record of my study carried out as requirements for the award of the degree of **Master of Engineering** in **CAD CAM** at **Thapar Institute of Engineering & Technology, Patiala** work carried out under the supervision and guidance of **Mr. A. S. JAWANDA, Associate Professor, Department of Mechanical Engineering, Thapar Institute of Engineering & Technology, Patiala.** This matter embodied in this report has not been submitted in part or full to any other university or institute for the award of any degree.

Navdeep Kumar.

Date: 28-Aug-2018

(Navdeep Kumar)
851381002

This certifies that the above declaration made by the student concerned is correct to the best of my knowledge & belief.

Jawanda 28/8/2018

Mr. A.S. JAWANDA

Associate Professor
Mechanical Engineering Department
Thapar Institute of Engineering & Technology, Patiala-147004

ACKNOWLEDGMENT

I would like to express a deep sense of gratitude and thank profusely to my teacher **Ajayinder Singh Jawanda** for their sincere & invaluable guidance, suggestions and attitude, which inspired me to submit thesis report in the present form. Their dynamism and diligent enthusiasm have been highly instrumental in keeping my spirits high. Their flawless and forthright suggestions blended with an innate intelligent application have crowned my task with success.

I would like to thank **New Mech-Fab Engineering Works Saharanpur U.P.** for valuable advice, thoughts and constant encouragement through discussions.

I would like to thank MED faculty for support and guidance who took a keen interest in my report and allowed me to access facilities of Mechanical Engineering Department laboratories. I am thankful to the Thapar Institute of Engineering & Technology for allowing me to analysis the stand structure in their premises.

A special thanks to my friends Azad Kumar, Maya Ram Yadav and Rohit Chopra for their help and support during thesis work.

NAVDEEP KUMAR

(851381002)

ABSTRACT

Stands used in stadia and sports arenas are usually fixed as a part of the civil work. There is a need for portable stands for an event like concerts, outdoor play and entertainment event for which construction of non-portable stand are expensive. Even compact stadium used in University and academic institutions are multi-purpose for which non-portable stand takes a valuable space. There is a need for foldable stand which can be stored remotely and installed quickly on occasions when events are staged. A foldable portable stand was fabricated using SS202 (Stainless Steel) material. The aim of the present study is to improvement and validation of the structural design for portable stand. The design was analyzed for structural strength for the requirement of seating capacity. The structure was analyzed under experimental loading conditions and its behavior simulated in CAD using Pro-Engineer/Creo and ANSYS 14.5 software. Validation of the simulation was done against experimental results. The critical stresses observed at joints were analyzed by simulating the joints as a kinematic member and validated through loading experiments as fabrication of only the joints.

Contents

LIST OF FIGURE

LIST OF TABLES

Chapter 5: Results and discussions

LIST OF ABBREVIATIONS

FEA	Finite element analysis
FBD	Free body diagram
IGES	Initial graphic exchange specification
SS	Stainless Steel
ASTM	American Society for Testing and Material
AISI	American Iron and Steel Institute
FOS	Factor of Safety

Chapter 1

Introduction

1.1 Introduction

Steel frames are used widely in sports arenas, household, industries and agricultural sector etc. Stainless Steel usually a choice when constructing a structural frame because of its excellent properties like as high strength and corrosion resistance.

Stainless steel portable stand structure sited in Thapar Institute of Engineering and Technology, Patiala for the purpose of sporting events as shown in figure 1.1. An existing stand is a large welded structure, consist of various elements having different shapes like as hollow square and rectangular cross-section beam. The material used for this portable stand is SS 202 and fabricated with the help of welding process. The portable stand was fabricated without considering any design parameter and structural analysis so there is a need to study the previous design.

(a) (b)

Figure1.1: (a) Stainless Steel Stand (b) Collapsible portable stand

1.2 Problem definition

During service, any static structure is subjected to stresses due to load. Due to this load, the strength of the frame able to withstand with load need to find which include safety and comfort of the user. All these parameters are involved in manufacturing procedures during the production stage.

A foldable portable stand frame is examined with respect to load, seating capacity, impact load when persons sitting on higher level seats would step down or jump down to the lower level in the process of vacating the stand. Also, we have to understand that how many people can sit on it as the heavy load can damage the joints and stand structure.

There is a number of different parameters which suited good for the analysis of the structure, but because of the complexity of the structure, only a few parameters have been chosen. In this project the basic geometry of the frame is not changed.

1.3 Specifications and constraint for Stand

- **Specification**
    - Stand designed for 16 people
    - Stand used for sporting arena
    - Collapsible portable stand
    - Rustproof
- **Constraints**
    - Number of people sitting four in a row
    - Casters wheel used
    - Theftproof

1.4 Objective of the Present Work

The objective of the present work is to improve the existing design of a portable stand. This study was focused on issues associated with modeling and testing of joints and stand structure. The primary purpose of this study was to develop technical information for strength and design of joints used in the frame. The study was intended to investigate and improve the FOS of stand frame. The following complementary objectives comprise the purpose of the study:

The key issue taken up during the proposed work are as follows:

- To investigate the mechanical properties of SS202

- To fabricate the stand joints by the welding process.
- To find the deflection of different stand base, seats and joints.
- Modeling of stand structure, joints and simulate with the help of FEA.
- To validate the FEA results against experimental results.
- Define Factor of Safety (FOS) to the portable stand.

1.5 Organization of Thesis

The organization of the thesis is given below:

Chapter 2 contains a review of the literature that is relevant to this research project. The review is intended to give an overview of weldability, structural analysis and footprints. The literature being introduced and discussed at the relevant stage of the thesis.

Chapter 3 begins with the study of existing design to find out the actual strength of the Stand joint and Stand structure under static load. Material test carried out as part of a study to find material strength.

Chapter 4 describes the modeling of Stand joints and Stand structure with the help of Pro-Engineer/Creo and ANSYS software used to discuss the load capacity of the Stand structure.

Chapter 5 presents results and discussion. All the results validated and give optimize view to experimental study and define the factor of safety.

Chapter 6 presents the conclusion of the thesis with the results is discussed and further directions in which the work can be extended are given.

Chapter 2

Literature Review

2.1 Literature Review

Manufacturing of the portable stand prototype expensive and time-consuming for this Computer Aided Engineering (CAE) play a very important role. One of the major roles of the CAE is reduced the number of the prototype to manufacturing by replacing them with simulation. It is easy to operate for designers and it reduces mental stress on the designer. In this, a prototype of the folding stand was implemented on a Computer and Finite Element Stress Analysis performed.

An interface needed that actively support CAE beginner users to perform analyses. ANSYS software used to analyze the any structure **[Miyoshi et al., 1999].** The modeling of the geometry deals with variable cross-sectional geometries. CAE quickly analyzed and give results according to our input. The prototype can be refined according to stress results. If we increasing cross-sectional geometries and member thickness, it can reduce stress on the joint areas but realize that the overall weight of the structure increases **[Karaoglu and Kuralay, 2002].** FEA used to get better results to this high-quality meshing used. High-quality meshing is very time-consuming process for building finite element model from CAD **[Liu et al., 2009].** Critical regions are determined in the structure which undergoes the stresses by applying finite element analysis. Using FEA the location of the failure can be predicted **[Topac et al., 2009].**

ANSYS can be used for structural analysis. It used to analyze the model and identify with hot spots. This hot spot is failure point of the experiment **[Wang et al., 2008].** Stress analysis using finite element method carried to determine the maximum stress value and its location on the structure. We can also reveal that the location of maximum stress and maximum deflection agrees with the theoretical maximum location of the simple beam under uniformly distributed load **[Nor et al., (2012].**

The structural stiffness of a structure is simulated by CAE software and structure design parameter are optimized. Structure stiffness can be affected by various geometrical parameters such as material property, the thickness of the sheet metal. It is necessary to establish a relation between geometric parameters and structural stiffness that expressed the larger vale of deflection.

Structure stiffness can also be related to material deflection if more deflection then lesser structure stiffness **[Li et al., 2014].**

When we fabricated the structure, welding is essential as it connects frames to each other. The welding parameter plays a determinant role in the structure of the strength **[Ye et al., 2007].** A structure, when used in actual loading conditions maximum stresses occurred at joints or contact with the bolt **[Xu et al., 2011; Pavlovic et al., 2015].** Any steel structure if fabricated with bolted T-stubs. It cannot sustain the initial damage from the loss of perimeter column **[Xu et al., 2011].** Stainless steel 202 structure fabricated by welding its metallurgical properties changed at the welded area so bead profile affects the strength and found that welded joint fabricated under vibratory condition get high tensile strength **[Sharma et al., 2014].** The geometry of the weld cannot be modeled in details because material properties vary over weld cross-section. There is a notch stress approach used R1MS, Radius 1 Maximum Stress **[Wang et al., 2008].**

AISI 202 SS has the similar mechanical properties as AISI 304 SS grade but SS 202 ability to resist corrosion is somewhat less as compare to SS 304 **[Bharwal and Vyas, 2014].** Rectangular box hollow cross section type section beam gives more strength as compared to C and I section beam. This rectangular section type beam also filled with diagonally so that the intermediate structure increases the strength of a rectangular hollow cross section **[Singh et al., 2014].**

When a person sitting on a bus or foldable stand, space that provided for legs very important as lesser space can hurt people legs so the size of the legs plays an important role. The size of the legs determined on the basis of data **[Salvendy, 2012].** Body weight with respect to footprints can also predict. Here size of the foot determined on the basis of data provided by **[Krishen, 2008; Hill et al., 2017].**

2.2 Summary of Literature Review

An overview of the key literature on the behavior and design of the stainless structures relevant to this thesis has been presented in this chapter. The discussions on the structure designs have been done. It is seen that several types of approaches can be followed to design a model.

Chapter 3

Study of Existing Design

3.1 Introduction

This chapter brings forth the details of existing design of a portable stand. The chapter describes the selection of material, material properties and strength of portable stand.

3.2 Material Selection

After a thorough literature survey it has been found that the selection of material for a Portable stand is depend upon the various factor like as application, functional properties (Mechanical and chemical), Manufacturing properties (Joining, Machining, Forming), availability and cost of material.

In the present study AISI 202 stainless steel is selected for the fabrication of Portable stand due to the following reasons:

- AISI 202 has a good combination of ductility and tensile strength.
- AISI 202 has good machinability and high corrosion resistance.
- AISI 202 has good formability and easily welded by different welding process.

The composition of base metal and mechanical properties from ASTM A240 is shown in table 3.1 and table 3.2 respectively.

Table 3.1: Composition of AISI 202

Element	Content
Carbon	≤0.15 %
Manganese	7.5-10.0 %
Phosphorus	≤0.060 %
Sulfur	≤0.030 %
Silicon	≤1 %
Chromium	17.0-19.0 %
Nickel	4.0-6.0 %
Nitrogen	≤0.25 %

Table 3.2: Mechanical properties of SS202

Density	7.7×10^3 kg m^{-3}
Hardness	241 HB
Elastic modulus	210 GPa
Yield strength	260 MPa
Tensile strength	620 MPa
Elongation	40 %
Poisson ratio	0.27–0.3

3.3 Bending test

This bend test used to determine the ductility of the material. For bending total three samples was made of material AISI 202 with ASTM specifications. Gradually load is applied on one face of the sample and evaluate deflection sustained by the material before crack initiated. Bending test specimens and bending machine setup shown in Figure 3.1 and 3.2 respectively. Figure 3.2 shows Gaps between the rollers were kept at 40 mm and punch size was 24 mm. The capacity of this machine is 1000 Ton.

Figure 3.1: Bending test Specimens

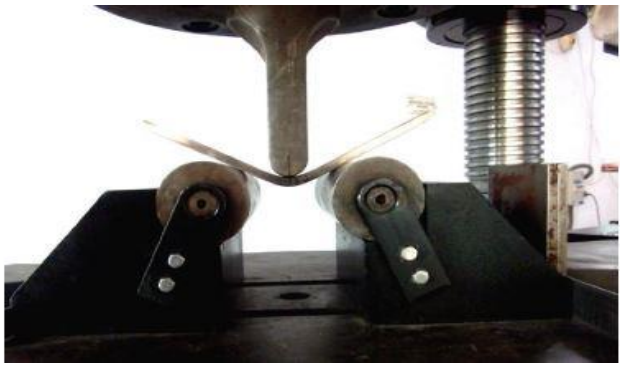

Figure 3.2: Bending machine setup

The bending test result is mentioned in Table 3.3 it explains the deflection with respect to the applied load.

Table 3.3: Maximum load for SS202

S.No.	Maximum bend load (KN)	Deflection (mm)
1	15.40	11.8
2	15.35	17.9
3	15.29	15.6

The mean value of the maximum bend load and deflection is 15.34 KN and 15.1 mm respectively. This bend test defines the deflection of the specimen with respect to gradually applied load.

Table 3.4: Bend sample of SS202 material after the test

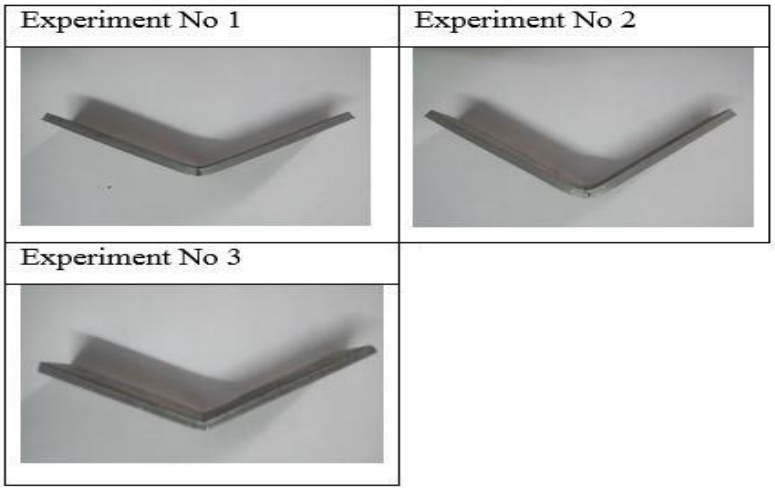

3.4 Tensile test

Material testing is important because the performance of a structure is frequently determined by the amount of deformation permitted. This tensile test performed in the universal testing machine with the gradually applied load. The specimen is subjected to controlled tension until failure occurs and find the tensile strength from stress-strain curves. Figure 3.3 and Figure 3.4 shows a schematic diagram of a tensile test specimen and actually fabricated specimen.

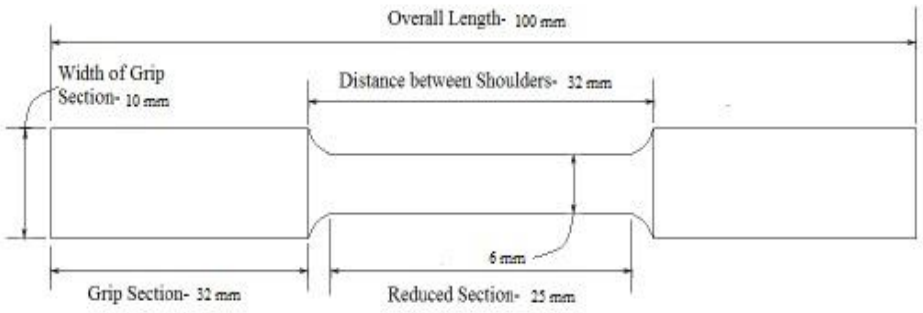

Figure 3.3: CAD design for tensile testing

Figure 3.4: Specimens for Tensile test

The tensile test used for determining the mechanical properties of the materials such as strength and Young's modulus. Tension test specimens mostly flat and round although specimen is prepared generally according to the ASTM specifications. Specimen subjected to stretching operation under static loading at a uniform rate in a universal testing machine. Stress is defined as the applied force divided by the original cross-sectional area. Engineering stress = (applied force)/(original area)= P/A0 and elongation of the sample is defined as strain. Engineering strain = (change in length)/(original length). Hooke's law is not valid beyond the yield point. The stress at the yield point is called yield stress, and is an important measure of the mechanical properties of materials. In practice, the yield stress is chosen as that causing a permanent strain of 0.002. Figure 3.4 shows the tensile test specimen which is tested in the universal testing machine. The calculated properties of material SS 202 are shown in Table 3.5.

Table 3.5: Material properties of SS202

Content	Properties
Material	SS 202
Tensile Strength	508 MPa
Yield Strength	249 MPa
Elastic modulus	204 GPa

3.5 Fabrication of Joints

A structure which is fabricated with joints and bolts then maximum stress occur at joints and bolts, it depends upon the geometry of the structure. It is important to investigate the joints and bolt strength of the structure **[Xu et al., 2011; Pavlovic et al., 2015].**

There is no option to find directly deflection of a portable stand joint but the first fabrication of joints separately and then applied static load. The universal testing machine used and calculate the deflection of a portable stand joint. The thickness of the sheet used for joint 1.5 mm. Metal Inert Gas (MIG) welding used to fabricate the joints. Voltage and current adjusted is 22 V and 180 A, respectively. In MIG welding, the filler material was used the similar composition of the base metal (SS202). In this study, AISI 202 wire of 2 mm diameter is used as filler metal. Total four experiment performed for each joint and mean value of four experiments at a particular load taken to further study. Mean value calculations of joints is shown in Appendix A.2, A.3, and A.4.

3.5.1 Fabricated joint1 link1

Figure 3.5(b) shows the fabrication of joint1 link1. A square pipe 51 mm with a hole 10.5 mm diameter is fabricated. A pin 10.5 mm is inserted in the hole and study the effect of the pin on the pipe under static applied load. The load is applied on a pin using another square pipe 47 mm and thickness 1.5 mm. Figure 3.5(c) shows that a square pipe with an inserted pin where another square pipe from upward direction inserted in it. The load is applied due to this deflection of the square pipe with a pin observed. The dimensions of the fabricated joint1 link1 are shown in Appendix A.2.

(a)

(b)

(c)

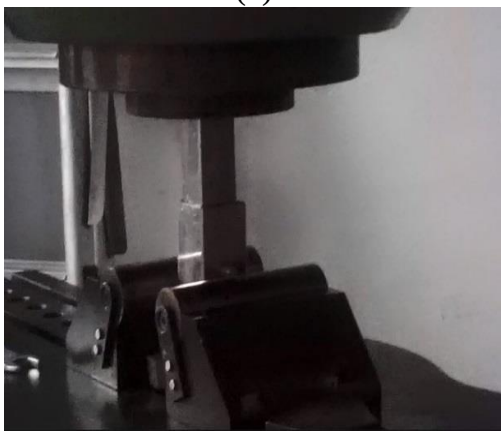

(d)

Figure 3.5: (a) Actual stand joint (b) Fabricated joint1 link1 (c) Load apply direction (d) Testing machine setup

Table 3.6: Results of joint1 link1 under static loading

Load (N)	Deflection(mm)
1000	0.0034
1500	0.0051
2000	0.0067
2500	0.0084

3.5.2 Fabricated welded joint1 link2

Figure 3.6(b) shows the fabrication of welded joint1 link2. In this welded joint1 link2, rectangular pipe 51 mm by 25.4 mm, 6 mm thickness plate and a pin 10.5 mm diameter is welded same as the actual stand joint which is used in the portable stand. The load is applied on a pin using another square pipe 47 mm and thickness 1.5 mm. The load is applied due to this deflection of the joint observed. The dimensions of the fabricated welded joint1 link2 are shown in Appendix A.3.

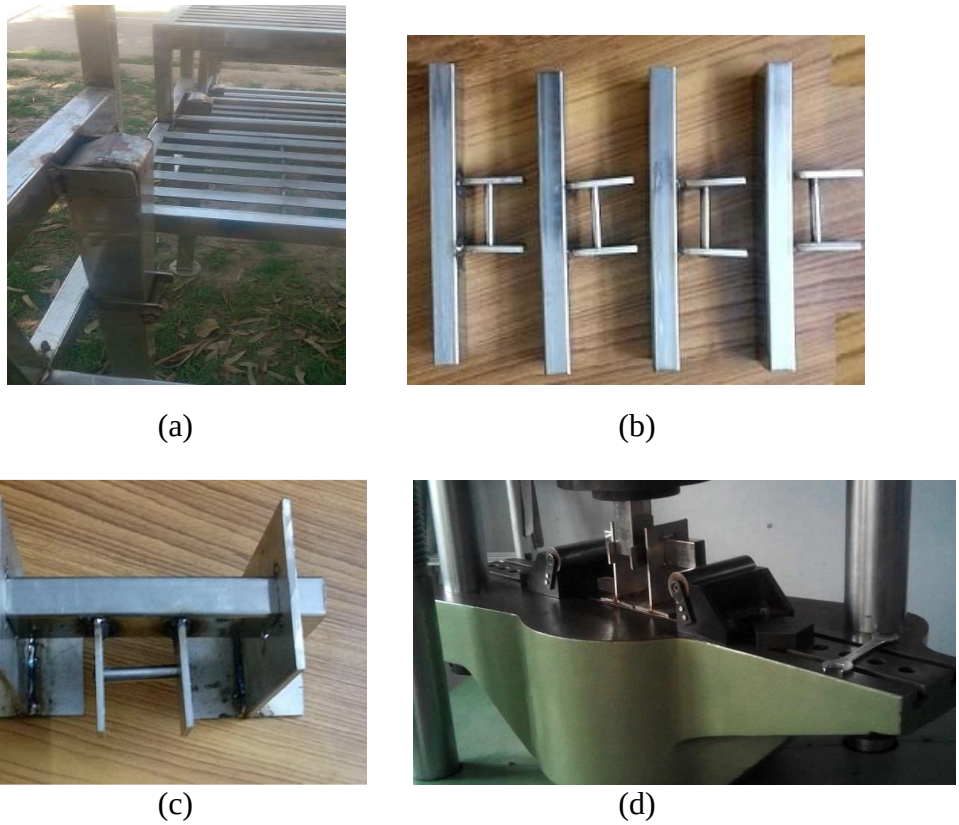

(a) (b)

(c) (d)

Figure 3.6: (a) Actual stand joint (b) Fabricated welded joint1 link2 (c) Fabricated joint setup (d) Testing machine setup

Table 3.7: Results of welded joint1 link2 under static loading

Load (N)	Deflection(mm)
1000	0.085
1500	0.125
2000	0.168
2500	0.216

3.5.3 Fabricated welded joint 2

Figure 3.7(b) shows the fabrication of welded joint2. In this joint, rectangular pipe 51 mm by 25.4 mm, 6 mm thickness plate and a pin 10.5 mm diameter is welded as a same actual stand joint which is used in the portable stand. The load is applied on a pin using another rectangular pipe 51 mm by 25.4 mm and thickness 1.5mm. The load is applied due to this deflection of the joint observed. The dimensions of the fabricated welded joint2 are shown in Appendix A.4.

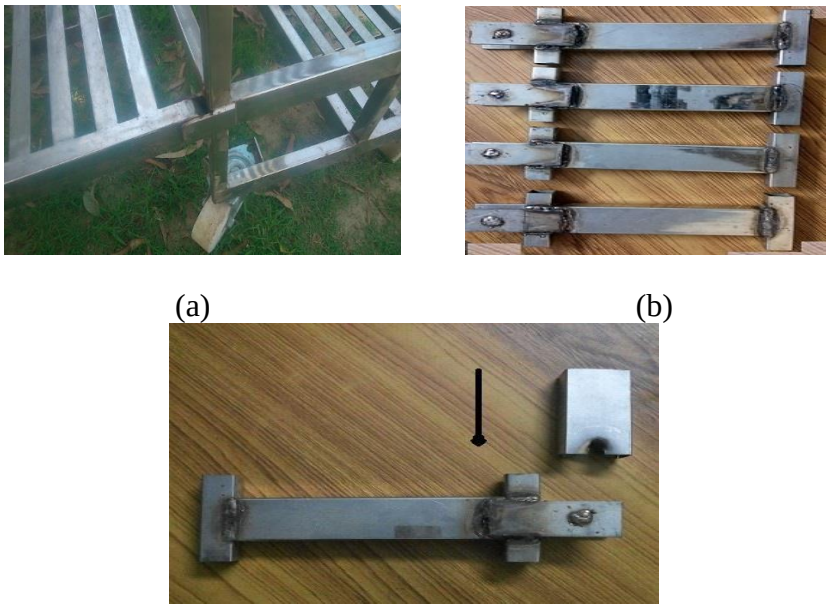

(a) (b)

(c)

Figure 3.7: (a) Actual stand joint (b) Fabricated welded joint2 (c) Load apply direction

Table 3.8: Results of welded joint2 under static loading

Load (N)	Deflection(mm)
1000	0.022
1500	0.034
2000	0.044
2500	0.055

3.6 Measure deflection of a stand under static applied load

A portable stand is a large welded structure. Its strength depends upon the material used and design of the structure. It is important to determine the stand deflection due to load. These experimental deflection results help us to validate the Finite Element Analysis (FEA) results.

Figure 3.8(a) shows that the actual portable stand which is tested for deflection. The stand is divided into four steps to analyze i.e. base1step1, seat1 step1, base2 step2 and seat2 step2 as shown in figure 3.8(b). A dial indicator is placed at the bottom of the portable stand which measures deflection under the applied load as shown in figure 3.8(d). Figure 3.8(c) shows that the load is applied using audience and due to this deflection measured in a dial indicator.

(a) (b)

(c) (d)

Figure 3.8: (a) Actual stand (b) Stand divide in four steps (c) Load applied
(d) Deflection measurement

Table 3.9: Audience weight

Person	Weight (kg)	Weight (N)
Person A	61.1	600
Person B	70	686.46
Person A'+B'	70+70	1372.93
Person A"+B"	70+60	1274.86
Person A"+B"+C"	70+85+71	2216.30
Person A'"+B'"+C'"	70+60+85	2108.42
Person A'"+B'"+C'"+D'"	83+80+76+90	3226.38
Person A""+B""+C""+D""	70+60+85+71	2804.7

3.6.1 Load applied for stand base1 step1

The load is applied to the base1 step1 in five different types as shown in table 3.10. When a human load of 686.46 N is applied, the resulting deflection measured using a dial indicator. All five experiments are done to check the deflection of the stand. The experiment is done under a loading condition of 600 N, 686.46 N, 1372.93 N, 2216.30 N and 3226.38 N.

Table 3.10: Load applied on base1 step1 under static loading

Experiment 1	Experiment 2
	
Experiment 3	Experiment 4
	

Table 3.11: Deflection due to audience weight for base1 step1

Audience Weight	Deflection(mm)
Person A	0.56
Person B	0.63
Person A'+B'	1.01
Person A"+B"+C"	1.38
Person A"'+B"'+C"'+D"'	1.54

3.6.2 Load applied for stand base2 step2

The load is applied to the base2 step2 in five different types as shown in table 3.13. When a human load of 600 N is applied, the resulting deflection measured using a dial indicator. All five experiments are done to check the deflection of the stand. The experiment is done under a loading condition of 600 N, 686.46 N, 1372.93 N, 2216.30 N and 3226.38 N.

Table 3.12: Load applied on base2 step2 under static loading

Experiment 1	Experiment 2
	
Experiment 3	Experiment 4
	

Table 3.13: Deflection due to audience weight for base2 step2

Audience Weight	Deflection(mm)
Person A	0.7
Person B	0.75
Person A'+B'	1.25
Person A"+B"+C"	1.69
Person A"'+B"'+C"'+D"'	1.92

3.6.3 Load applied for stand seat1 step1

The load is applied to the seat1 step1 in five different types as shown in table 3.15. When a human load of 600 N is applied, the resulting deflection measured using a dial indicator. All five experiments are done to check the deflection of the stand. The experiment is done under a loading condition of 600 N, 686.46 N, 1274.86N, 2108.42N and 2804.7N.

Table 3.14: Load applied on seat1 step1 under static loading

Experiment	Experiment 2
	
Experiment 3	Experiment 4
	

Table 3.14: Deflection due to audience weight for seat1 step1

Audience Weight	Deflection(mm)
Person A	0.79
Person B	0.89
Person A"+B"	1.41
Person A"'+B"'+C"'	2.04
Person A""+B""+C""+D""	2.31

3.6.4 Load applied for stand seat2 step2

The load is applied to the seat2 step2 in five different types as shown in table 3.17. When a human load of 600 N is applied, the resulting deflection measured using a dial indicator. All five experiments are done to check the deflection of the stand. The experiment is done under a loading condition of 600 N, 686.46 N, 1274.86N, 2108.42N and 2804.7N.

Table 3.16: Load applied on seat2 step2 under static loading

Experiment 1 	Experiment 2 
Experiment 3 	Experiment 4 

Table 3.17: Deflection due to audience weight for seat2 step2

Audience Weight	Deflection(mm)
Person A	0.76
Person B	0.86
Person A"+B"	1.38
Person A"'+B"'+C"'	2.01
Person A""+B""+C""+D""	2.25

3.7 Comparison of Joint and Stand deflection results

- Deflection plot of joints with varying load is shown in Figure 3.9. From the plots, it is observed that the maximum deflection observed is in the case of welded joint1 link2 it is because of its design and load applied. We can conclude that the deflection in joints1 link1, welded joint2 is less than the welded joint1 link2.

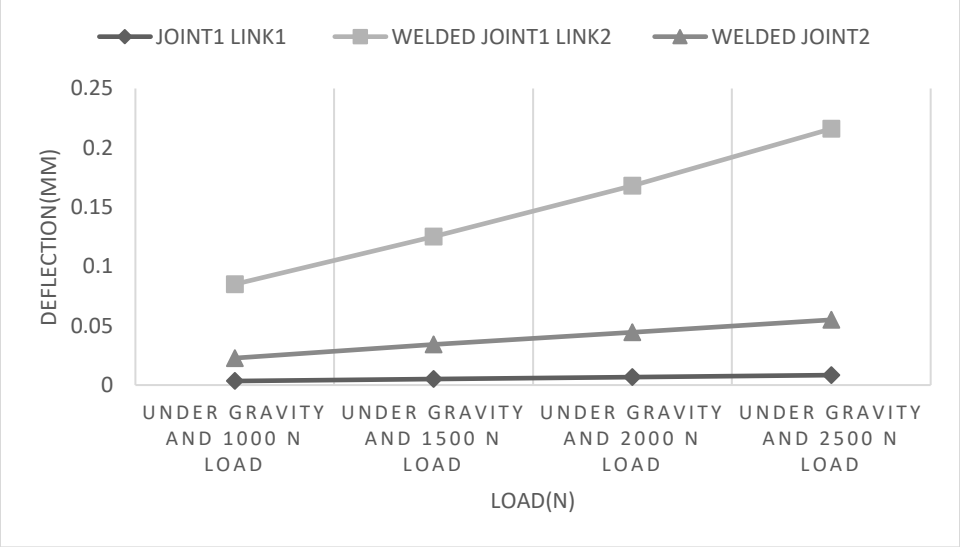

Figure 3.9: Graphical representation of joint1 link1, welded joint1 link2 and welded joint2

- Deflection plot with varying load is shown in Figure 3.10 and Figure 3.11. From the plots, it is observed that the maximum deflection observed is in the case of base2 step2. We can conclude that the deflection developed in base1 step1 is less than the base2 step2 because of base1 step1 support conditions i.e. fixed support. Seat1 step1 and seat2 step2 are also observed and maximum deflection in case of seat1 step1 and seat2 step2 almost same or varies with a very small margin. It is because of fixed support used in both cases same.

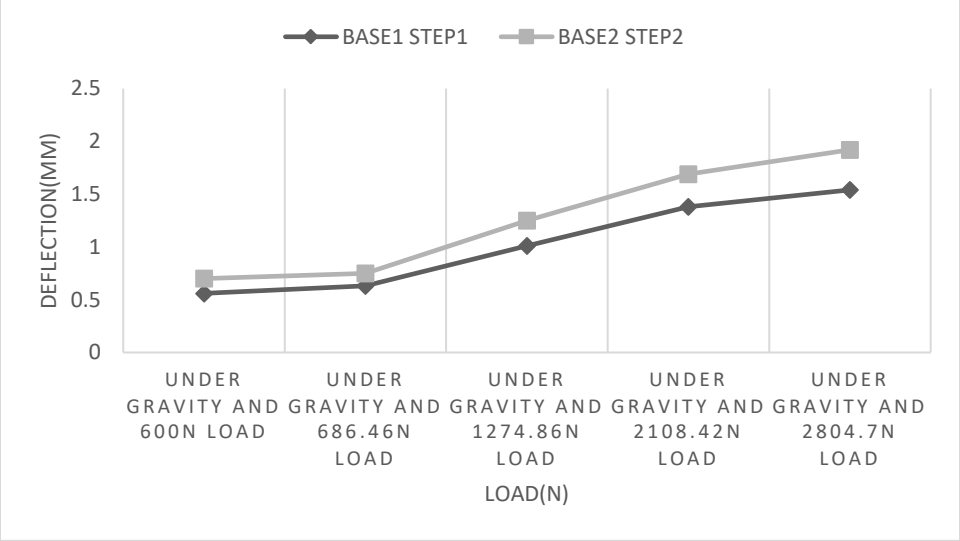

Figure 3.10: Graphical representation of base1 step1 and base2 step2 under static loading

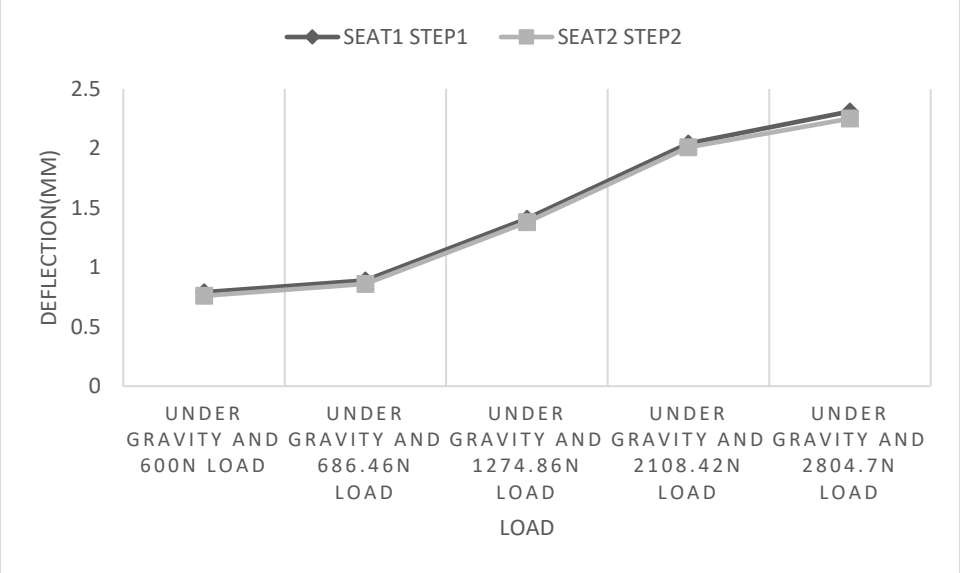

Figure 3.11: Graphical representation of seat1 step1 and seat2 step2 under static loading

3.8 Impact loading

When any structure designed we have to think about which way they can fail to avoid permanent failure. This can involve complex calculations but still, we can use engineering concept to ensure nothing unexpected happens. In this project, we took some assumptions and perform simple design calculations.

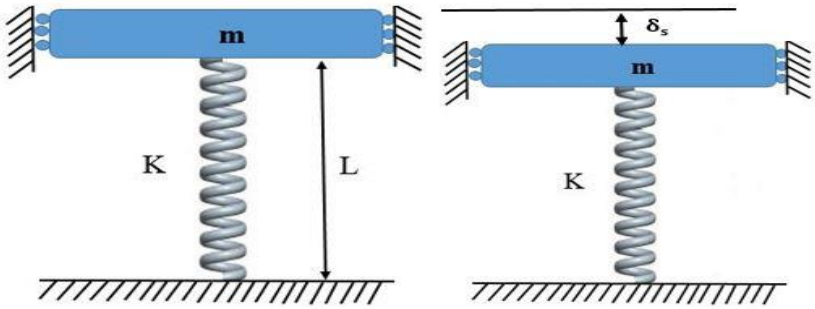

(a)

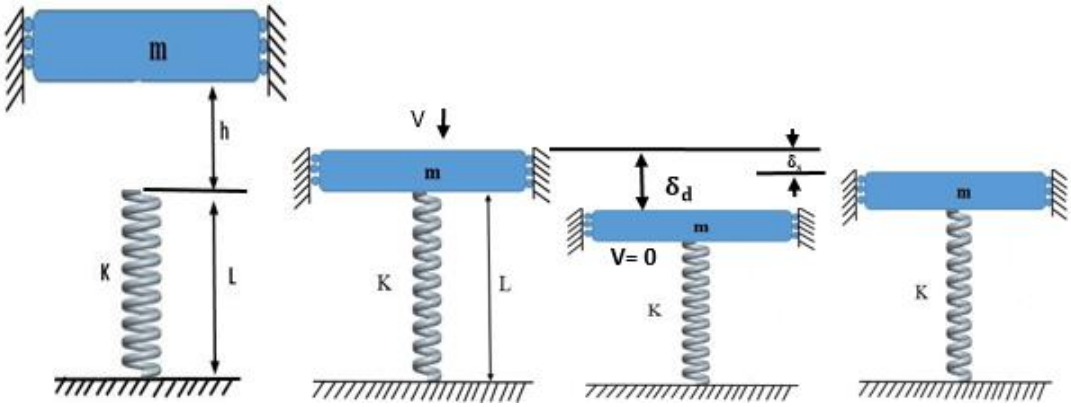

(b)

Figure 3.12: (a) Static deflection due to weight (b) Dynamics deflection due to weight

To define the impact force on a stand when weight strikes the stand at a certain height a dynamic deflection occurs and then a stand comes to a balanced position but due to this weight, static deflection still present there.

h = Height of dropped weight

w = Dropped weight

δ_s = Static deflection of the structure under the weight

δ_d = Dynamic deflection

K = Stiffness of the distributed mass system

F_s =Static force

F_d = Dynamic force

Dynamics Magnification Factor (DMF):

$$\mathrm{DMF} = \frac{\mathrm{F_d}}{\mathrm{F_s}} = \frac{\delta_\mathrm{d}}{\delta_\mathrm{s}} \tag{3.1}$$

$$\mathrm{DMF} = 1 + \sqrt{1 + \frac{2\mathrm{h}}{\delta_\mathrm{s}}} \tag{3.2}$$

Dynamics Magnification Factor with respect to dropped height and static deflection is shown in this equation **[West and Pakrashi, 2007].** We can predict that from this equation as static deflection increases DMF decreases. The calculation of DMF equations shown in Appendix A.6.

If h=0

$$\mathrm{DMF} = \frac{\mathrm{F_d}}{\mathrm{F_s}} = 2 \tag{3.3}$$

It means dynamics force is two times of static force.

For dynamic force:

$$\mathrm{F_d} = \mathrm{DMF\ x\ F_s} \tag{3.4}$$

3.9 Buckling analysis

When a straight column subjected to axial compression suddenly undergoes bending. Here buckling analysis study on the stand support which undergoes a buckling load.

Critical buckling load P_{cr} for columns is theoretically given as **[Case et al., 2013]**

$$\mathrm{P_{cr}} = \frac{\pi^2 \mathrm{EI}}{(\mathrm{KL})^2} \tag{3.5}$$

Where, I = moment of inertia about the axis of buckling

K = effective length factor based on end boundary conditions

If one end fixed and other end pin joined then K = 0.7 **[Case et al., 2013].**

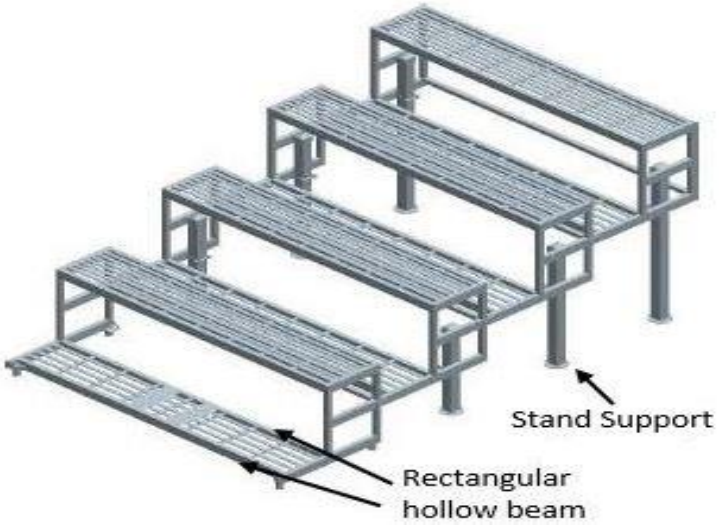

Figure 3.13: Stand square hollow section support and beam

Square Hollow Section (SHS) used here with 50.8 mm wide by 50.8 mm high by 1.5 mm thick and length 1000 mm.

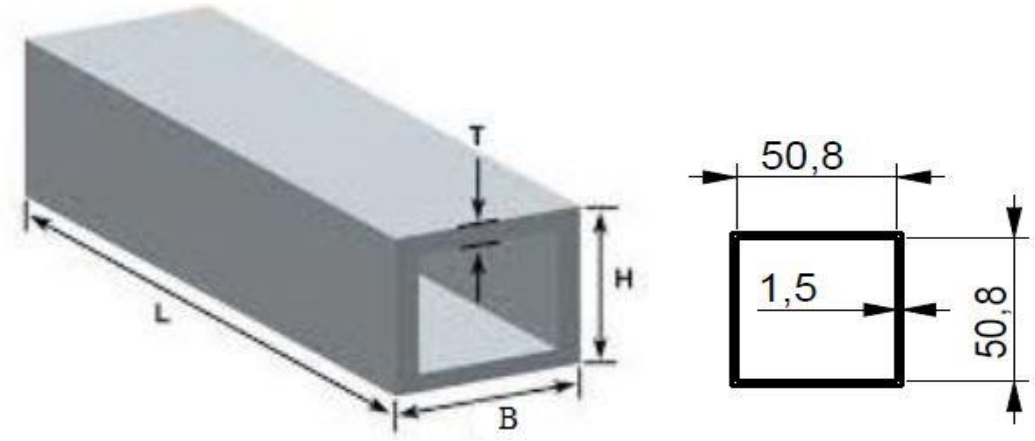

(a) (b)

Figure 3.14 (a) CAD model for support (b) cross sectional view of support

B = 0.0508 m, H = 0.0508 m

b = 0.0478 m, h = 0.0478 m

$$I = \frac{BH^3}{12} - \frac{bh^3}{12} \quad (3.6)$$

$I = 1.199\ x\ 10^{-7}\ m^4$

$P_{cr} = 506.64\ KN$

$$\text{Safe Compressive Load} = \frac{\text{Buckling load}}{\text{Factor of safety}} \quad (3.7)$$

$$\text{Safe Compressive Load} = \frac{506.64}{3}$$

$$\text{Safe Compressive Load} = 168.88\ KN$$

Now we know that safe compressive load for stand support beam is 168.88 KN. The calculation of buckling analysis equations shown in Appendix A.7.

3.10 Beam analysis

A rectangular hollow section type of beam used while fabricated the foldable stand. It's dimensioned 50.8 mm by 25.4 mm with 1.5 mm thickness and length 1500 mm. The calculation of beam analysis equations shown in Appendix A.8.

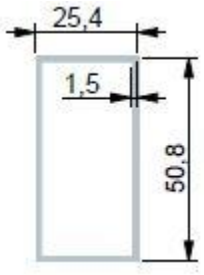

Figure 3.15 Rectangular hollow beam cross-sectional

$$I = \frac{BH^3}{12} - \frac{bh^3}{12} \quad (3.8)$$

B = 0.0254 m, H = 0.0508 m

b = 0.0224 m, h = 0.0478 m

$I = 7.36\ x\ 10^{-8}\ m^4$

Consider a simply supported beam i.e. fixed at both ends and point load applied on the center then maximum deflection is given as **[Case et al., 2013].**

δ_{max} = maximum deflection

$$\delta_{max} = \frac{WL^3}{48EI} \quad (3.9)$$

$$\delta_{max} = 2.72 \text{ mm}$$

3.11 Summary

This chapter put forward the design of the present study. The chapter makes the work plan and key issues that to be adapted to fulfill the objective of the work. This chapter discussed the procedure and design of experiment to fabrication of the stand joints. Joints and portable stand experiment results help us to validate the Finite Element Analysis (FEA) results.

Chapter 4

Finite Element Analysis

4.1 Methodology

This FEA technique is used to calculate the deflection of a portable stand and its joints. Force is applied at a particular location of a stand and joints. The basic principle of FEA is to the discretization of the model in small parts, means the structure is first divided into an equivalent system of many smaller bodies where two or more than two elements are interconnected with each other.

4.2 Modeling of Folding Stand

The modeling of a portable stand is done in Pro Engineer/Creo shown below Fig. 4.1. Modeling of a portable stand design is based on the design of the actual portable stand. The extension file of modeling software is .PRT converted into Initial Graphics Exchange Specification file format (IGES) so that it allows the digital exchange of information among Computer-aided design (CAD) systems.

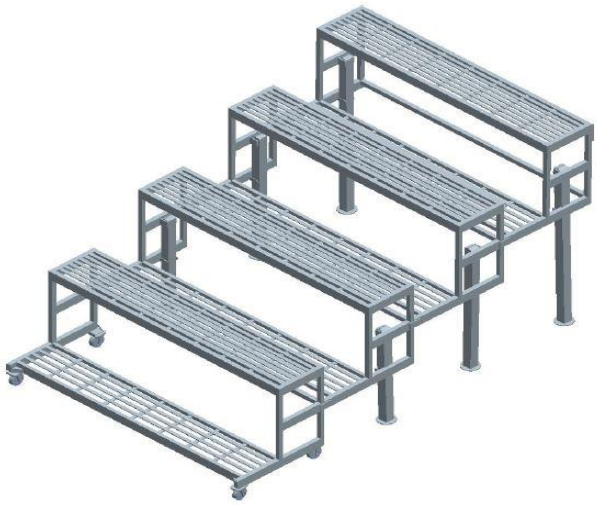

Figure 4.1: CAD model of the stand in Pro-Engineer/Creo

4.2.1 Modeling of welded stand joints

The modeling of joint1 link1, welded joint1 link2 and welded joint2 is done in Creo then import to the ANSYS software. The extension file of modeling software is .PRT converted into initial graphics exchange specification file format so that it allows to exchange of information among

computer-aided design. The modeling of joints is based on the actual joints used in the experimental study.

i) Modeling of welded joint 1

- **Modeling of joint1 link1**

Figure 4.3 shows that the modeling of joint1 link1. A pin 10.5 mm is inserted in the hole and study the effect of the pin on the square pipe under static applied load. The load is applied on a pin using another square pipe with thickness 1.5 mm. Figure 4.2 shows that location and zoomed view of the joint1 link1.

Figure 4.2: Zoomed view of joint1 link1

Figure 4.3: Actual view of joint1 link1

- **Modeling of Welded joint1 link 2**

Figure 4.5 shows that the modeling of welded joint1 link2. Modeling of this joint done as same parameter which is used in actual portable stand. The load is applied on a pin due to this deflection of the joint observed. The dimensions of the welded joint1 link2 same as fabricated joint. Figure 4.4 shows that location and zoomed view of the welded joint1 link2.

Figure 4.4: Zoomed view of welded joint1 link2

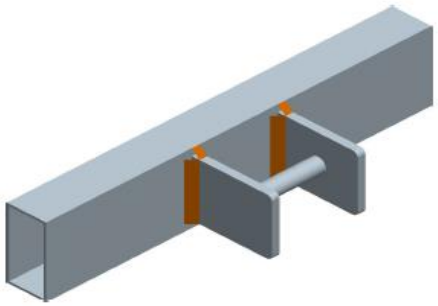

Figure 4.5: Actual view of welded joint1 link2

ii) Modeling of Welded joint 2

Figure 4.7 shows that the modeling of welded joint2. Modeling of this joint done as same parameter which is used in actual portable stand. The load is applied on a pin due to this deflection of the joint observed. The dimensions of the welded joint2 same as fabricated joint. Figure 4.6 shows that location and zoomed view of the welded joint2.

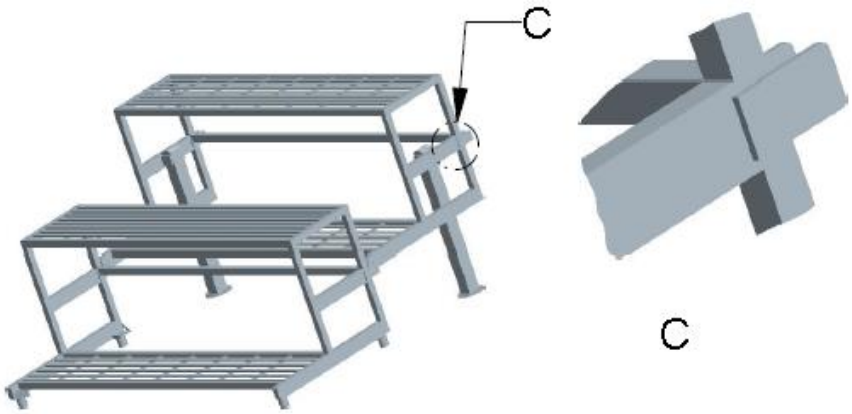

Figure 4.6: Zoomed view of welded joint2

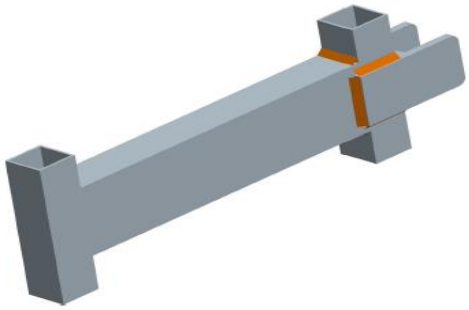

Figure 4.7: Actual view of welded joint2

4.2.2 Interface between modeling software and analysis software

A file needed to communicate between the two different software. Analysis software help to overcome this problem by directly reading the part files produced by the Creo. The modeling of a portable stand is done in the modeling software and import modeling software file into analysis software through IGES file format. Simply the modeling software file is saved in IGES extension and then import into analysis software.

Modeling is also possible in ANSYS software but the reason to draw in Creo software is that due to the complexity of the geometry. Due to fewer modeling tools available in the analysis software. Modeling is not so powerful in ANSYS software as compared to other mechanical modeling software.

4.2.3 Material properties of stand

The strength of material which deals with the behavior of the solid objects subjected to stresses and strain. The stresses acting on the material causes deformation of the material. This deformation is called the strain of the material.

The material properties of the modeling portable stand are taken experimental values which are calculated by the tensile test of the material. Using these values it help to validate the FEA results with experimental results. Some material properties used same as ASTM A240 like Density, Poisson ratio. Calculated material properties which used in modeling of the portable stand and joints are shown below in Table 3.4.

Table 4.1: Mechanical properties of SS202

Tensile yield strength	249 MPa
Tensile ultimate strength	508 MPa
Young's modulus	204 GPa

4.2.4 Meshing of stand and joints

The Pro-Engineer geometric model is imported into ANSYS for meshing. Meshing is a very important part of finite element modeling. For the more accurate result of the solution at an appropriate number of locations, refinement of meshing is very important but due to this number of meshing element increases. The greater number of an element requires more computer resources like memory and processing time. The quality of mesh is defined on the basis of elements and complexity of the geometry. In the area of a high geometric complexity, mesh element become destroyed. The poor quality element can lead to poor results or in some cases no results.

In FEA, Stand joint used a default and automatic mesh because of its complexity but some refinement done in the area where the boundary condition is applied. The figure 4.8 shows the comparison between automatic mesh and mesh after refinement. After refinement, elements and nodes on the stress area increased. It helps to keep more accurate results.

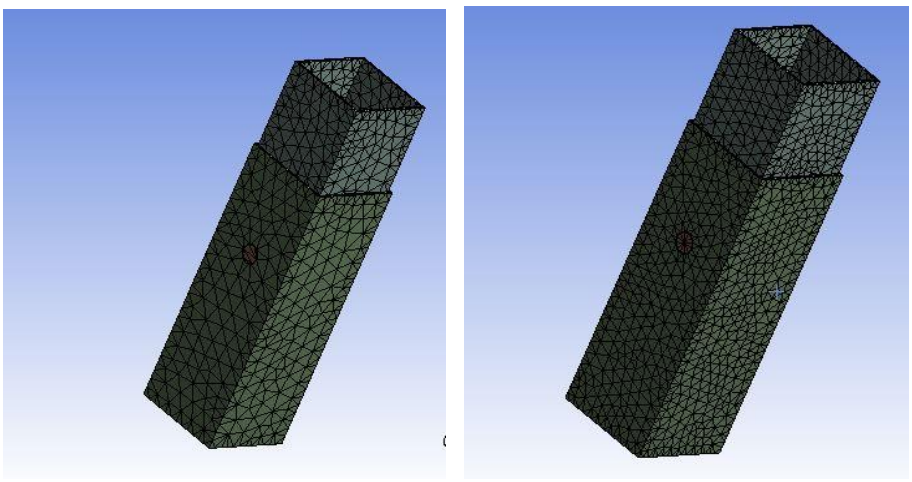

(a) (b)

Figure 4.8: Meshing of the joint (a) before refinement and (b) after refinement

4.2.5 Boundary conditions

Defining boundary condition involves the location of the boundaries on the basis of the model. The data required at a boundary depends upon the boundary conditions type and physical model. In this model boundary conditions are forces direction and fixed support discussed.

- **Forces**

In a physical model of portable stand different type of forces acting which has a major impact as the deflection. Figure 4.9 shows that forces direction applied on the joints and structure.

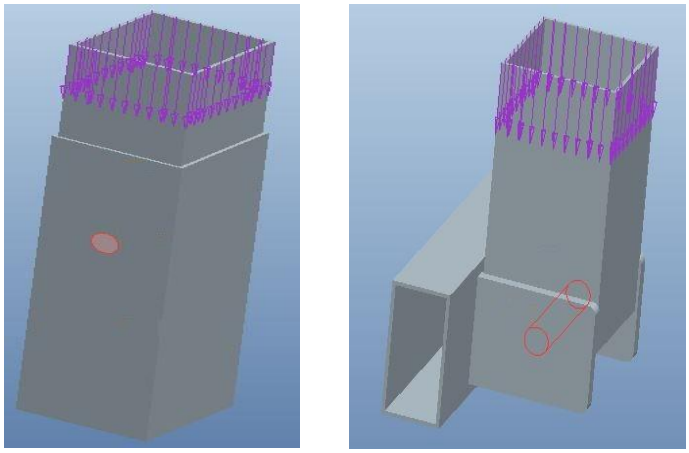

(a) (b)

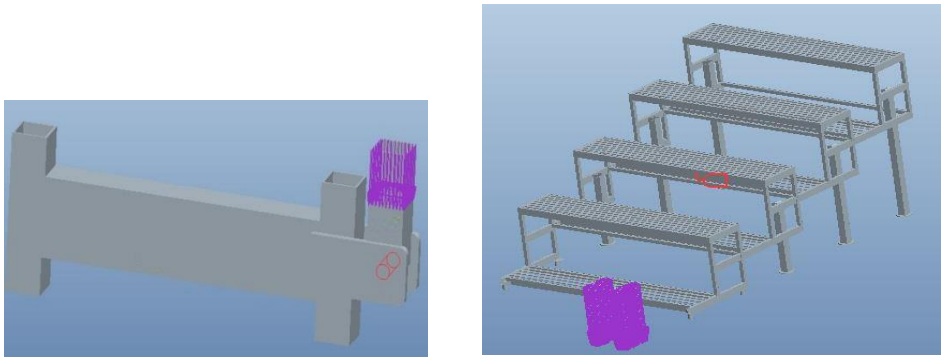

(c) (d)

Figure 4.9: Force direction applied to joints and structure

- **Fixed support**

The model is fixed from different locations according to our requirements. Joints and model fixed support as shown in Figure 4.10.

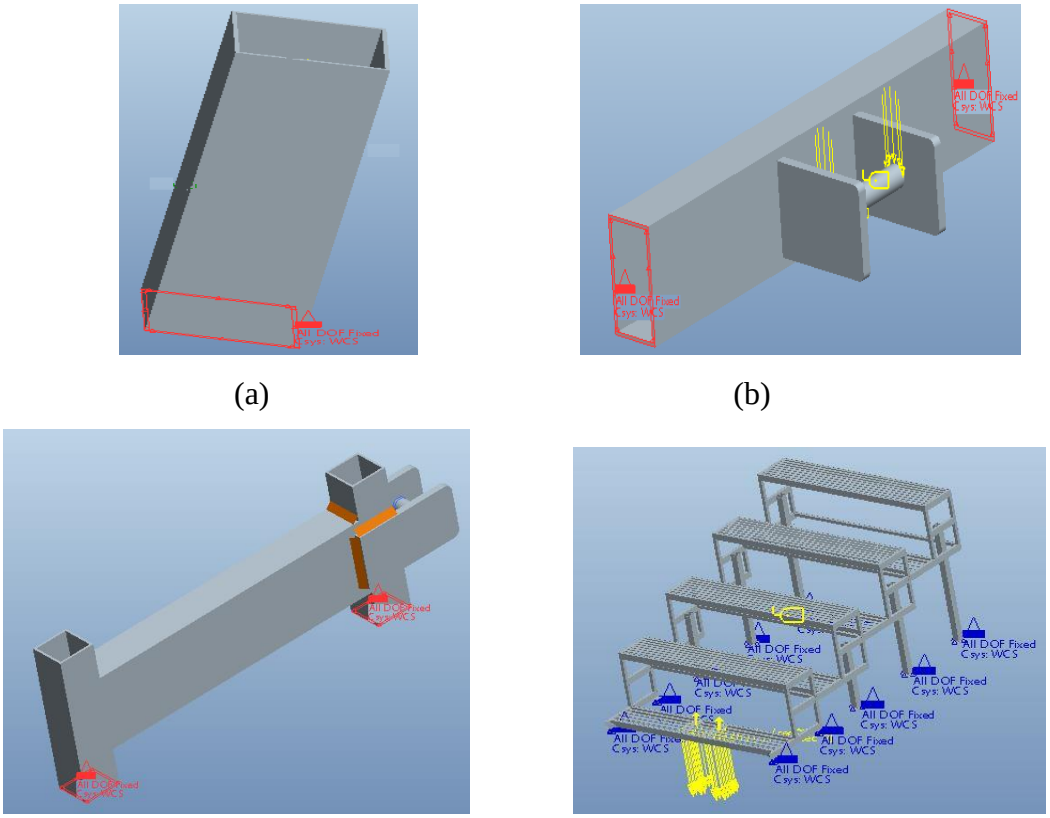

(a) (b)

(c) (d)

Figure 4.10: Fixed support applied to joints and structure

4.2.6 Simulation

The next stage of the FEA process is the static analysis. The FEA conducts a series of computational procedures involving applied forces and the properties of the elements which produce a model solution. Such a structural analysis allow the determination of effects such as deflections and stresses which are generated by applied structural loads such as the force.

4.2.7 Post processing

Post process is the image of results. To identify the boundary condition and identify the effect of these conditions can be studied by using the image of results. Representation of data i.e. Numerical and graphical helps to identify the failure and prediction of results.

4.3 Results and Analysis

In this Force is applied vertically downward compressed and configuration of joints is shown in figures. The gravity in –y direction is applied to the structure and joints. One analysis is done under gravity only to check the stress and deflection of the structure. Four more analyses are done under a different loading. During all four analyses joint is under the effect of gravity load as well. The stress and deflection of the joints are noted in each analysis and are listed in tables.

4.3.1 Deflection and stress due to force for joint1 link1

Figure 4.11 shows a load of 1000 N which is applied at pin surface 10.5 mm diameter with the help of a square pipe 47 mm with 1.5 mm thickness. When a load of 1000 N is applied in presence of gravity, the resulting deflection and stress of the joint are shown in table 4.2. Deflection of the rectangular pipe with the pin is measured. Figure 4.12(a) and figure 4.12(b) shows that the maximum stress and zoomed view of the joint where maximum stress has occurred.

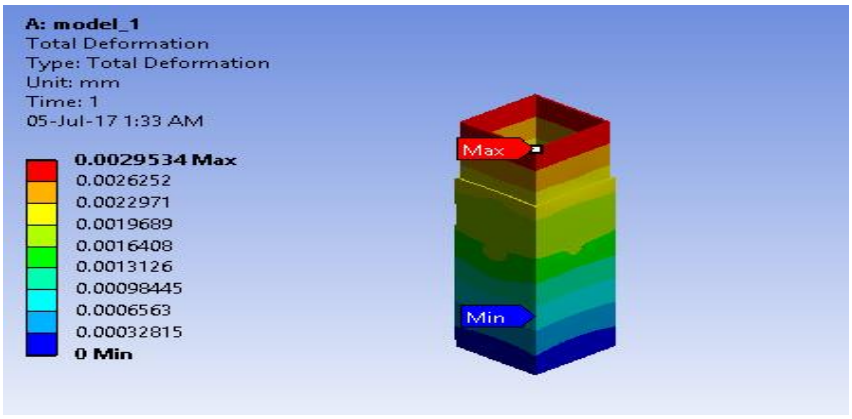

Figure 4.11: Deflection of joint1 link1

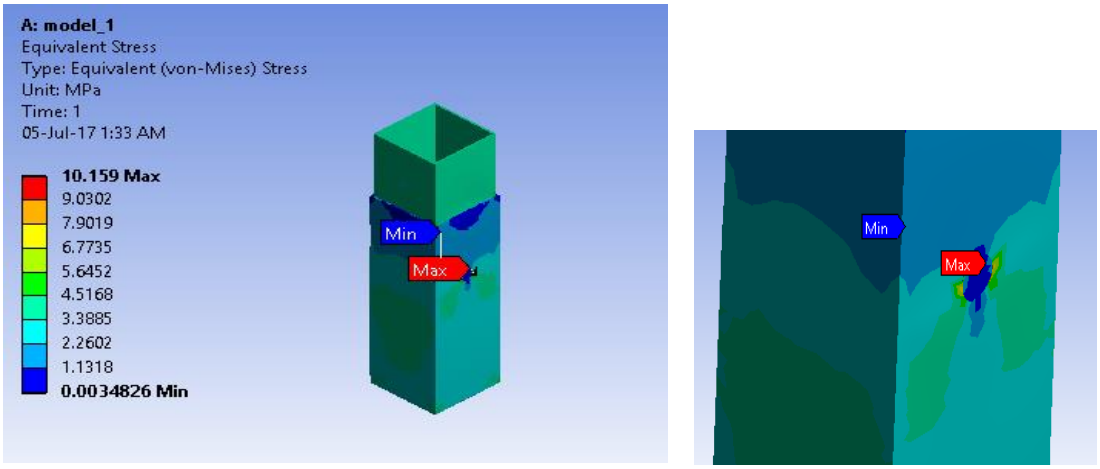

(a) (b)

Figure 4.12: (a) Stress of Joint1link1 (b) Zoomed view of maximum stress

Table 4.2: Results of Joint1 link1 under different loading

	Deflection (mm)	Stress (MPa)
Under gravity and 1000 N load	0.0029	10.159
Under gravity and 1500 N load	0.0044	15.216
Under gravity and 2000 N load	0.0058	20.273
Under gravity and 2500 N load	0.0073	25.33

4.3.2 Deflection and stress due to force for welded joint1 link2

Figure 4.13 shows a load of 2500 N which is applied at pin surface 10.5 mm diameter with the help of a square pipe 51 mm with 1.5 mm thickness. When a load of 2500 N is applied in presence of gravity, the resulting deflection and stress of the joint are in table 4.3. Figure 4.14(a) and figure 4.14(b) shows that the maximum stress and zoomed view of the joint where maximum stress has occurred.

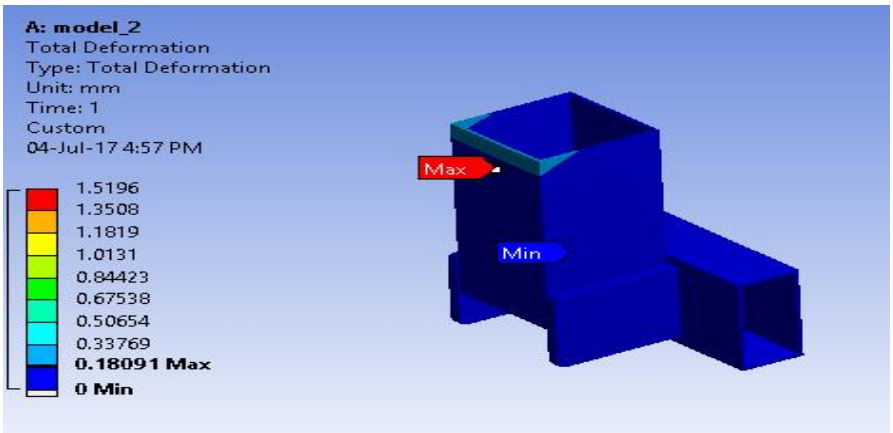

Figure 4.13: Deflection of welded joint1 link2

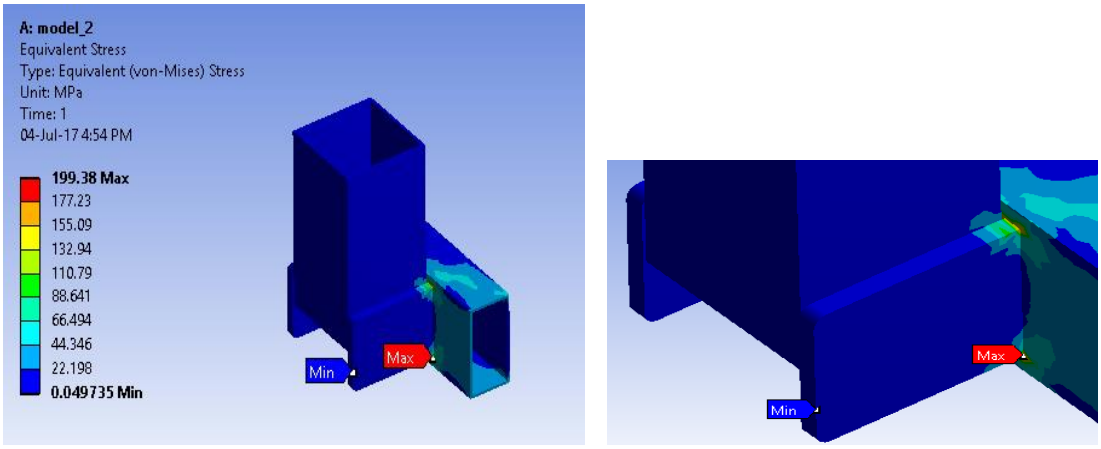

(a) (b)

Figure 4.14: (a) Stress of welded joint1 link2 (b) Zoomed view of maximum stress

Table 4.3: Results of welded joint1 link2 under different loading

	Deflection (mm)	Stress (MPa)
Under gravity and 1000 N load	0.07236	79.75
Under gravity and 1500 N load	0.10854	119.63
Under gravity and 2000 N load	0.14472	159.5
Under gravity and 2500 N load	0.18091	199.38

4.3.3 Deflection and stress due to force for welded joint2

Figure 4.15 shows a load of 1000 N which is applied at pin surface 10.5 mm diameter with the help of a square pipe 25.4 mm with 1.5mm thickness. When a load of 1000 N is applied in presence of gravity, the resulting deflection and stress of the joint are shown in table 4.4. Figure 4.16(a) and figure 4.16(b) shows that the maximum stress and zoomed view of the joint where maximum stress has occurred.

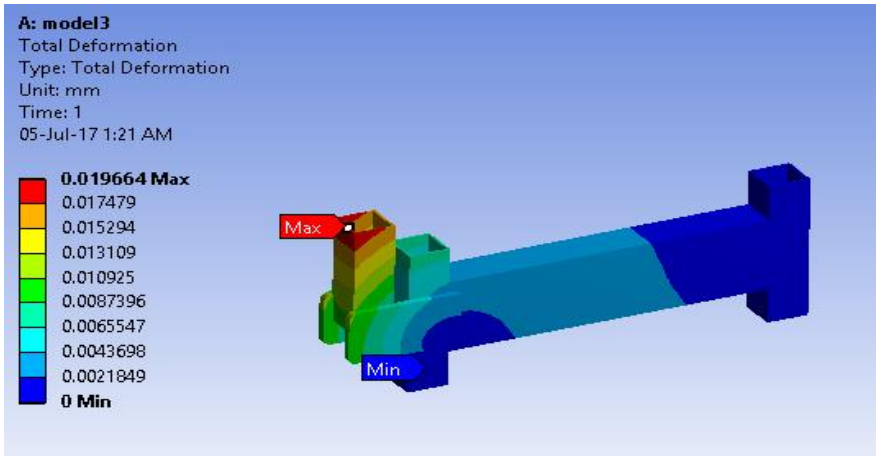

Figure 4.15: Deflection of welded joint2

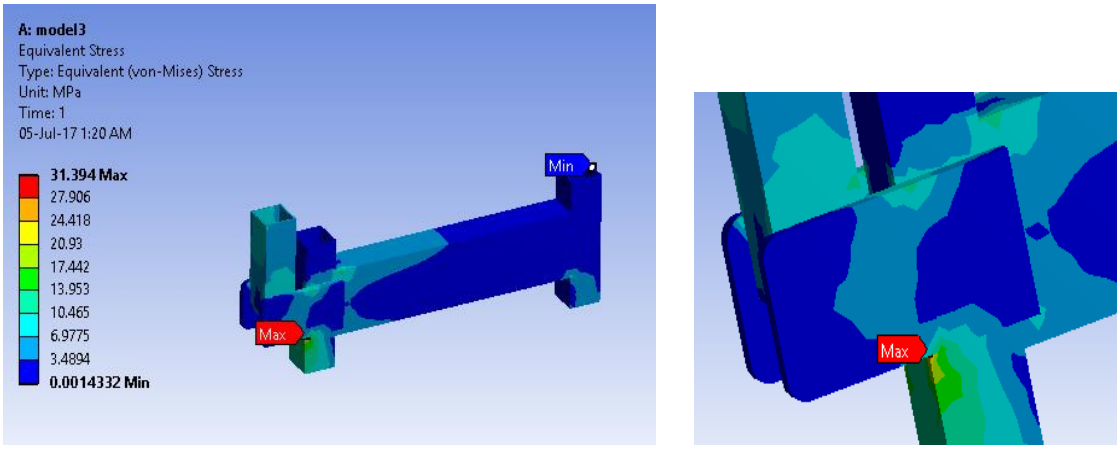

(a) (b)

Figure 4.16: (a) Stress of welded joint2 (b) Zoomed view of maximum stress

Table 4.4: Results of welded joint2 under different loading

	Deflection (mm)	Stress (MPa)
Under gravity and 1000 N load	0.01966	31.39
Under gravity and 1500 N load	0.02949	47.09
Under gravity and 2000 N load	0.03932	62.78
Under gravity and 2500 N load	0.04916	78.48

4.3.4 Comparison of all joints results combined

The deflection plot of all three joints with variation in load is shown in Figure 4.17. From the plot, it has seen that the maximum deflection observed is in the case of welded joint1 link2. We can conclude that the deflection developed in joints1 link1, welded joint2 is less than the welded joint1 link2 because of its structure and load distribution. Experimental and FEA results shows that the same as maximum deflection at welded joint1 link2.

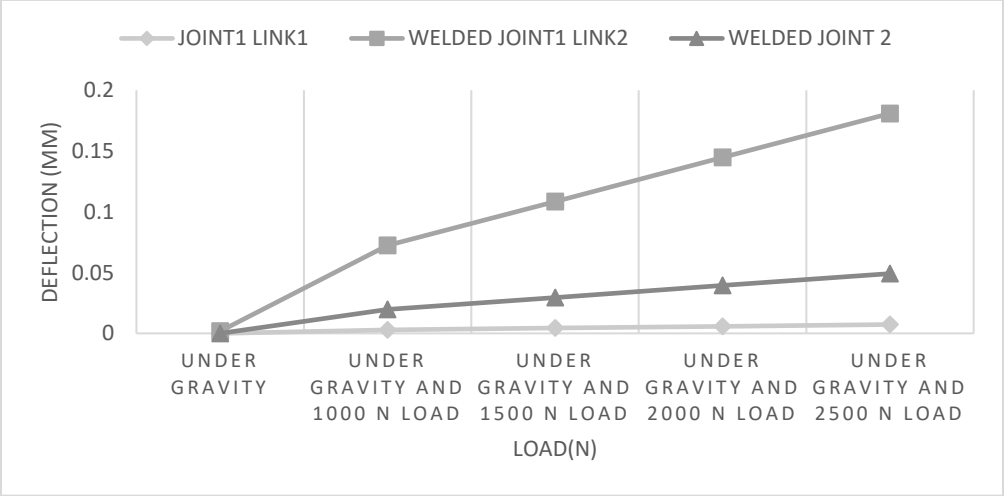

Figure 4.17: Plot of Deflection versus Load for joint1 link1, welded joint1 link2, welded joint2

4.3.5 Deflection and stress due to load on the full model

Figure 4.18 shows that portable stand geometry. In this applied load in four different surfaces and according to this deflection and stress noted. The load applied to these surfaces according to the load applied physically.

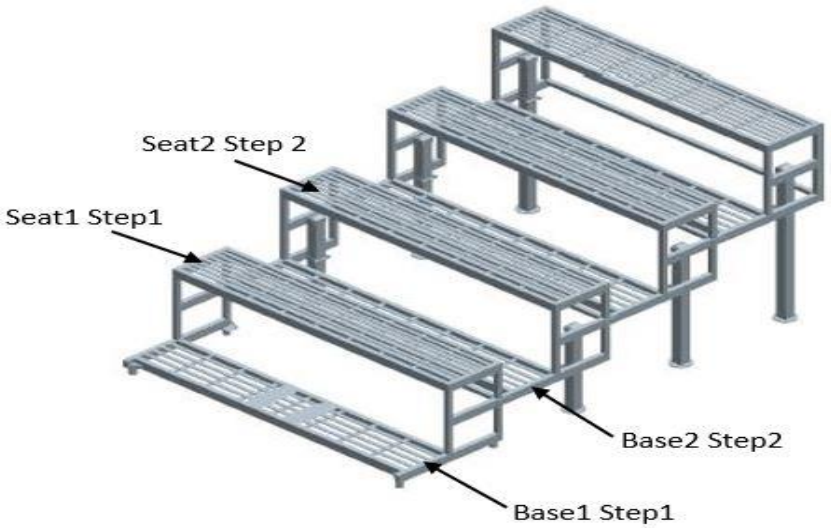

Figure 4.18: CAD model for portable stand

Figure 4.19 shows a load of 686.46 N which is applied to a particular area i.e. two surfaces the same as a human footprint. When a load of 686.46 N divided into two parts equally and applied in presence of gravity, the resulting loading surface and stress of the folding stand shown in Figure 4.19(a) and Figure 4.19(b) respectively.

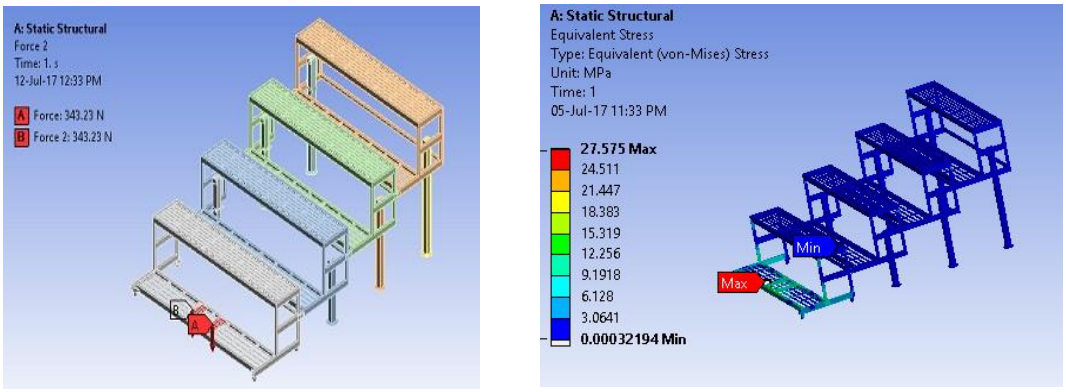

(a) (b)

Figure 4.19: Portable stand static loading (a) Loading at particular area (b) Maximum stress

Table 4.5 defines that stand loading area in four different type.

One person	Two person
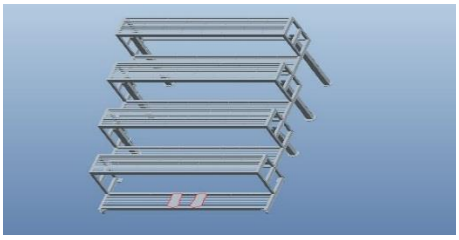	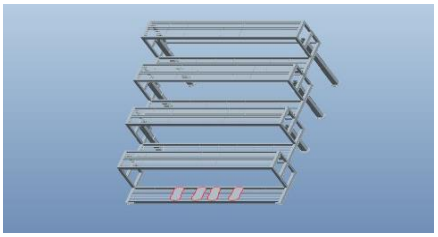
Three person	**Four person**
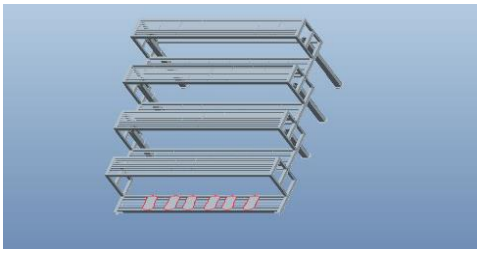	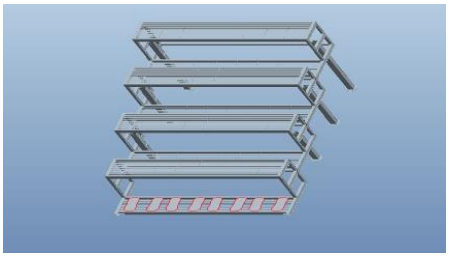

Body weight defines a strong and positive correlation with the various measures of the footprint. Footprints also inductive the body size of the person **[Krishan, 2008]**. Footprint size is taken to get the measurement so we can use it in CAD model during loading conditions.

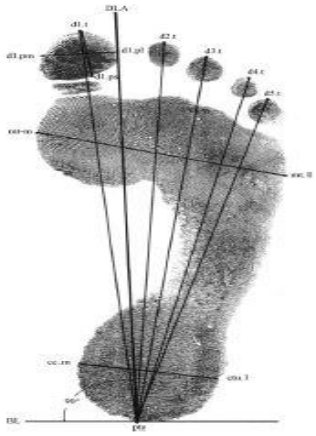

Figure 4.20: Landmarks and measurement on the footprint [**Krishan, 2008**]

4.3.6 Deflection and stress for base1 step1 due to force

Figure 4.21 shows a load of 686.46 N which is applied at stand defined surface base1 step1. When a load of 686.46 N divided into two parts equally and applied in presence of gravity, the resulting deflection and stress of the portable stand are shown in Figure 4.21(a) and Figure 4.21(b) respectively. All five analysis is done under the gravity to check the stress and deflection of the

stand. Analyses are done under a loading condition of 600 N, 686.46 N, 1372.93 N, 2216.30 N and 3226.38 N which applied in –y direction at the defined surface of the stand.

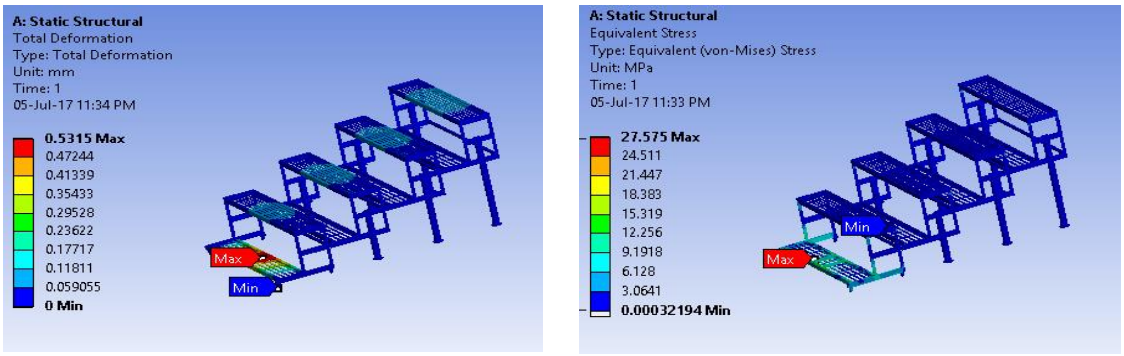

(a) (b)

Figure 4.21: Simulation results by FEA for base1 step1 (a) Total deflection (b) Maximum stress

Table 4.6: Results of stand base1 step1 under static loading

	Deflection (mm)	Stress (MPa)
Person A	0.47	24.3
Person B	0.5315	27.575
Person A'+B'	0.8446	46.227
Person A"+B"+C"	1.1219	61.975
Person A"'+B"'+C"'+D"'	1.2263	71.565

4.3.7 Deflection and stress for base2 step2 due to force

Figure 4.22 shows a load of 2216.30 N which is applied at stand defined surface base2 step2. When a load of 2216.30 N divided into six parts equally and applied in presence of gravity, the resulting deflection and stress of the portable stand are shown in Figure 4.22(a) and Figure 4.22(b) respectively. All five analysis is done under the gravity to check the stress and deflection of the stand. Analyses are done under a loading condition of 600 N, 686.46 N, 1372.93 N, 2216.30 N and 3226.38 N which applied in –y direction at the defined surface of the portable stand.

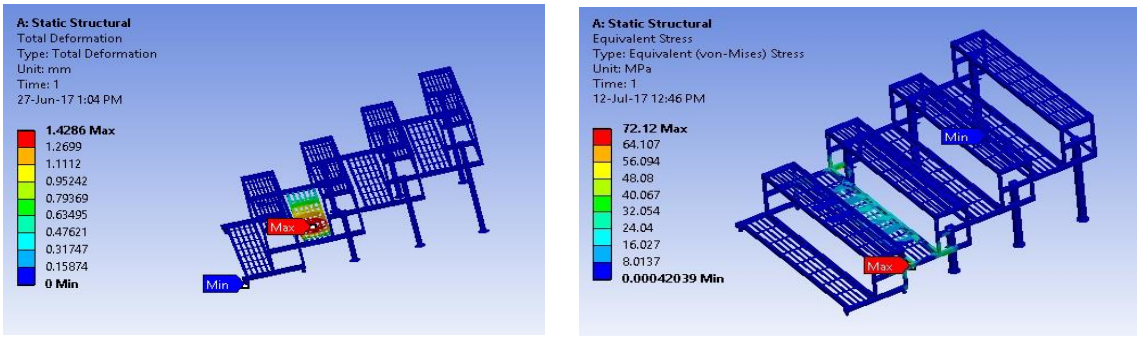

(a) (b)

Figure 4.22: Simulation results by FEA for base2 step2 (a) Total deflection (b) Maximum stress

Table 4.7: Results of stand base2 step2 under loading

	Deflection (mm)	Stress (MPa)
Person A	0.58	30.79
Person B	0.66	35.08
Person A'+B'	1.06	51.06
Person A"+B"+C"	1.428	72.12
Person A"'+B"'+C"'+D"'	1.588	83.87

4.3.8 Deflection and stress for seat1 step1 due to force

Figure 4.23 shows a load of 1274.86 N which is applied at stand defined surface seat1 step1. When a load of 1274.86 N divided into six parts equally and applied in presence of gravity, the resulting deflection and stress of the portable stand are shown in Figure 4.23(a) and Figure 4.23(b) respectively. All five analysis is done under the gravity to check the stress and deflection of the stand. Analyses are done under a loading condition of 600 N, 686.46 N, 1274.86 N, 2108.42 N and 2804.7 N which applied in –y direction at the defined surface of the portable stand.

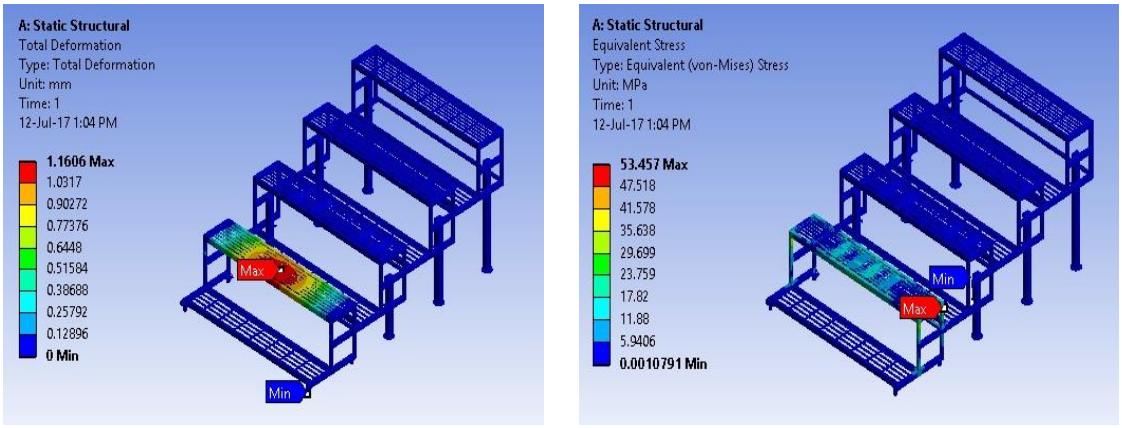

(a) (b)

Figure 4.23: Simulation results by FEA for seat1 step1 (a) Total deflection (b) Maximum stress

Table 4.8: Results of stand seat1 step1 under loading

	Deflection (mm)	Stress (MPa)
Person A	0.68	29.038
Person B	0.77	32.58
Person A"+B"	1.16	53.457
Person A"'+B"'+C"'	1.66	79.874
Person A""+B""+C""+D""	1.844	91.8

4.3.9 Deflection and stress for seat2 step2 due to force

Figure 4.24 shows a load of 2108.42 N which is applied at stand defined surface seat2 step2. When a load of 2108.42 N divided into six parts equally and applied in presence of gravity, the resulting deflection and stress of the portable stand are shown in Figure 4.24(a) and Figure 4.24(b) respectively. All five analysis is done under the gravity to check the stress and deflection of the stand. Analyses are done under a loading condition of 600 N, 686.46 N, 1274.86 N, 2108.42 N and 2804.7 N which applied in –y direction at the defined surface of the portable stand.

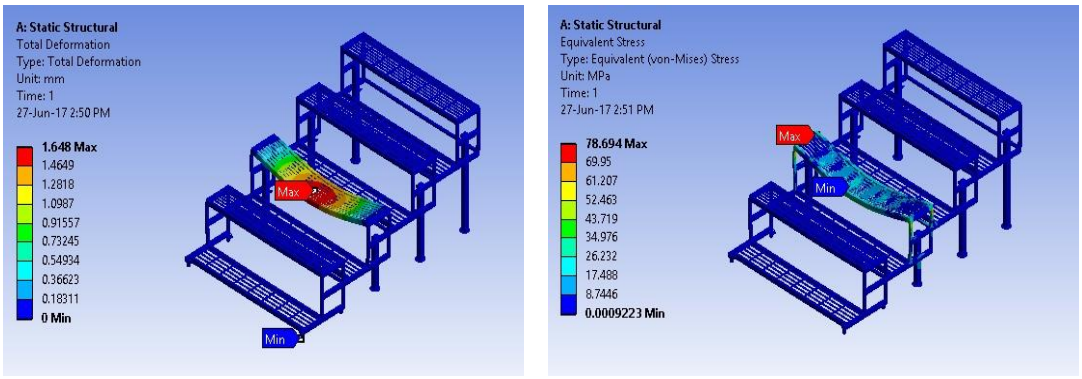

(a) (b)

Figure 4.24: Simulation results by FEA for seat 2 step2 (a) Total deflection (b) Maximum stress

Table 4.9: Results of stand seat2 step2 under static 1oading

	Deflection (mm)	Stress (MPa)
Person A	0.677	28.635
Person B	0.76	32.136
Person A"+B"	1.216	56.0
Person A"'+B"'+C"'	1.648	78.69
Person A""+B""+C""+D""	1.82	90.209

4.3.10 Comparison of results for base1 step1 and base2 step2

Deflection plot with varying load is shown in Figure 4.25. From the plots, it is also observed that the maximum deflection observed is in the case of base2 step2. We can conclude that the deflection developed in base1 step1 is less than the base2 step2. It is because of support used in both bases different each other.

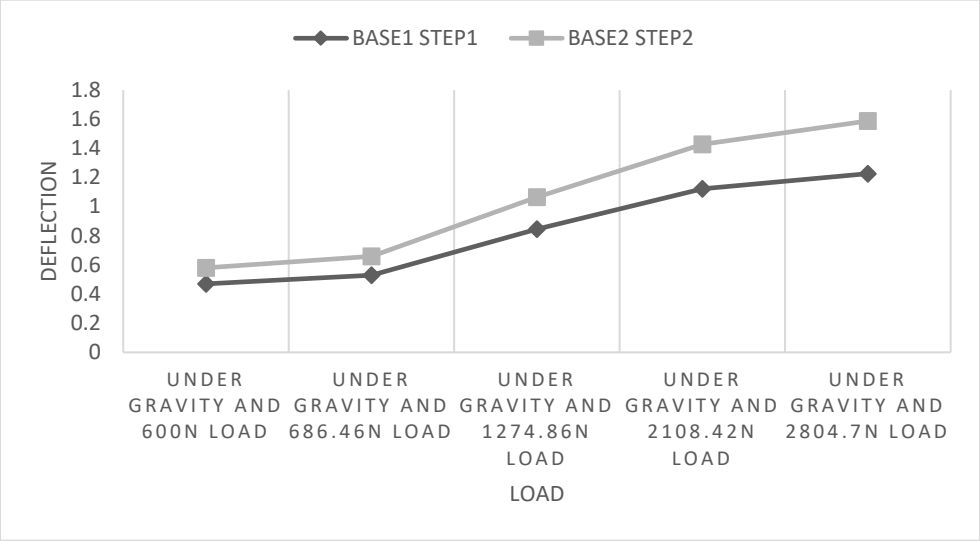

Figure 4.25: Graphical representation of deflection with a load for base1 step1 and base2 step2 combined

4.3.11 Comparison of results for seat 1 step1 and seat2 step2

Deflection plot with varying load is shown in Figure 4.26. From the plots, It is also observed that the maximum deflection in case of seat1 step1 and seat2 step2 almost same or varies with very small margin. We can conclude that the deflection developed in seat1 step1, seat2 step2 almost same because support used in seats same.

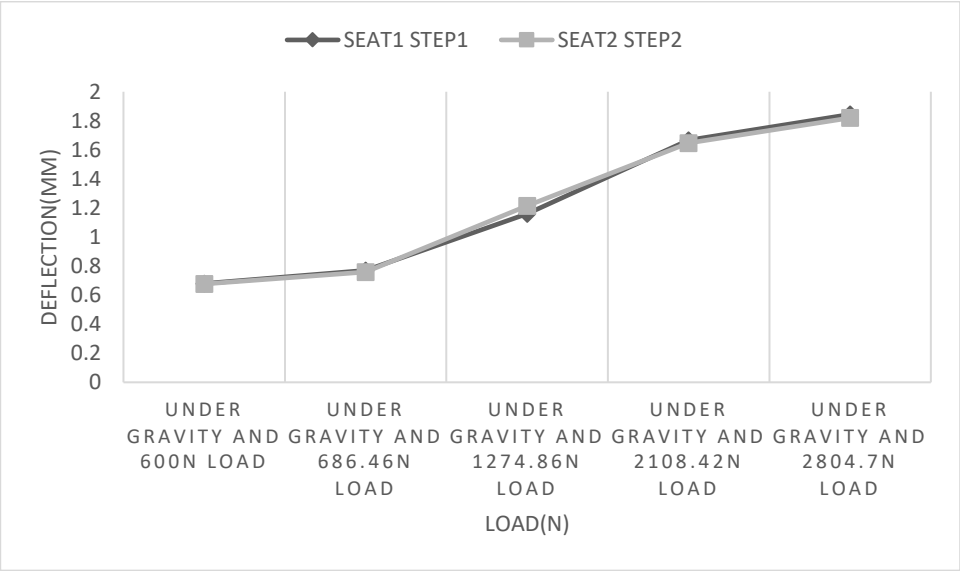

Figure 4.26: Graphical representation of deflection with a load for seat1 step1 and seat2 step2 combined

4.4 Summary

In this chapter joints and stand have been tested in static loading. The static analyses of all the joints have been performed using ANSYS and the results have been tabulated. Form the results it has been seen that deflection occurs more in the welded joint1 link2 as compare to joint1 link1 and welded joint2. In portable stand analysis, it is observed that base2 step2 get more deflection than base1 step1 because of support conditions. Seat1 step1 and seat2 step2 deflection almost same as both cases support conditions are same.

Chapter 5

Results and Discussions

5.1 Introduction

This chapter deals with the validation of FEA results with experimental results. It is possible by comparing the simulation results with the corresponding experimental finding. The percentage difference is noted between them and this percentage difference used later in the simulation. This percentage difference helps us to find the exact strength of the portable stand in the simulation. The percentage difference is used a further redesign of the portable stand to increase FOS.

5.2 Validation of joint simulation using a measuring quantity deflection

All joints are tested using a universal testing machine with the static applied load then deflection is measured. ANSYS software is used to get FEA result i.e. stress and deflection. FEA results are validated with respect to experimental results and noted the percentage difference between them. This percentage difference used to get stress values by adding percentage difference.

Percentage difference comes because the composition of material can be different. The material composition used for tensile test and portable stand can be different as both the material cast at the different time and different company. It is a possibility that tensile test results that we got maybe vary with the actual portable stand. It is not possible to cut material from the portable stand and used for testing.

5.2.1 Validation of joint1 link1

Table 5.1 shows that the percentage difference between experimental and FEA results of joint1 link1. Figure 5.1 shows that all experimental results greater than FEA results. Maximum value of percentage difference 14.70 and minimum is 13.09.

Table 5.1: Validation of joint1 link1

Load (N)	Experimental (mm)	FEA (mm)	Percentage Difference
1000	0.0034	0.0029	14.70
1500	0.0051	0.0044	13.72
2000	0.0067	0.0058	13.43
2500	0.0084	0.0073	13.09

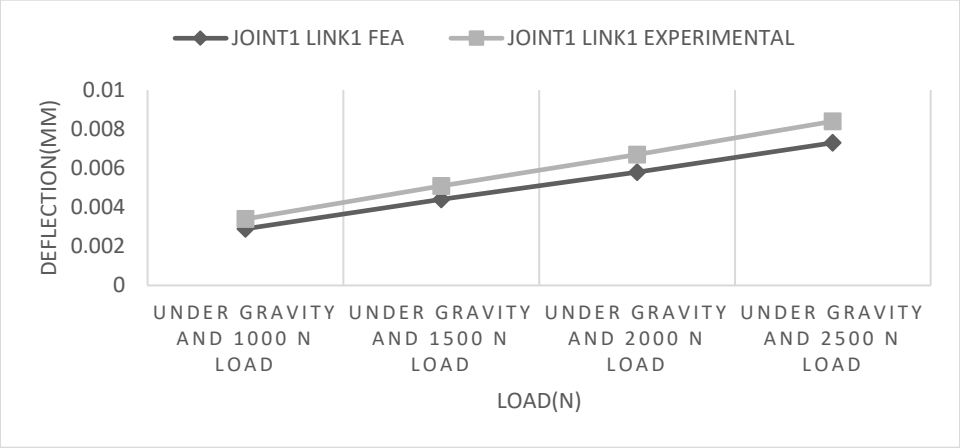

Figure 5.1: Graphical representation of Joint1 link1 FEA and Experimental

5.2.2 Validation of welded joint1 link2

Table 5.2 shows that the percentage difference between experimental and FEA results of welded joint1 link2. Figure 5.2 shows that all experimental results greater than FEA results. Maximum value of percentage difference 14.70 and minimum is 12.45.

Table 5.2: Validation of welded joint1 link2

Load (N)	Experimental (mm)	FEA (mm)	Percentage Difference
1000	0.085	0.0724	14.70
1500	0.125	0.1085	13.20
2000	0.168	0.1447	13.86
2500	0.216	0.1809	12.45

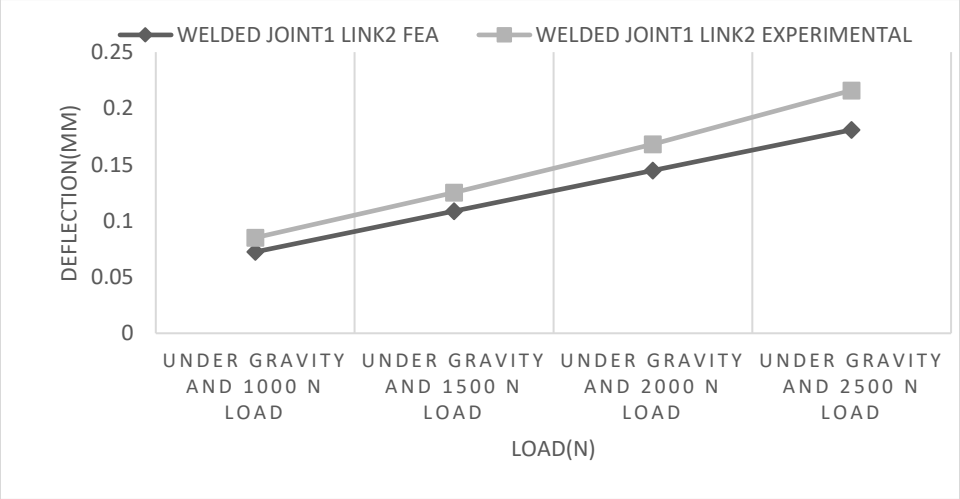

Figure 5.2: Graphical representation of welded Joint1 link2 FEA and Experimental

5.2.3 Validation of welded joint2

Table 5.3 shows that the percentage difference between experimental and FEA results of welded joint2. Figure 5.3 shows that all experimental results greater than FEA results. Maximum value of percentage difference 13.90 and minimum is 10.54.

Table 5.3: Validation of welded joint2

Load (N)	Experimental (mm)	FEA (mm)	Percentage Difference
1000	0.0227	0.0197	13.65
1500	0.0343	0.0295	13.90
2000	0.0445	0.0394	11.46
2500	0.0550	0.0492	10.54

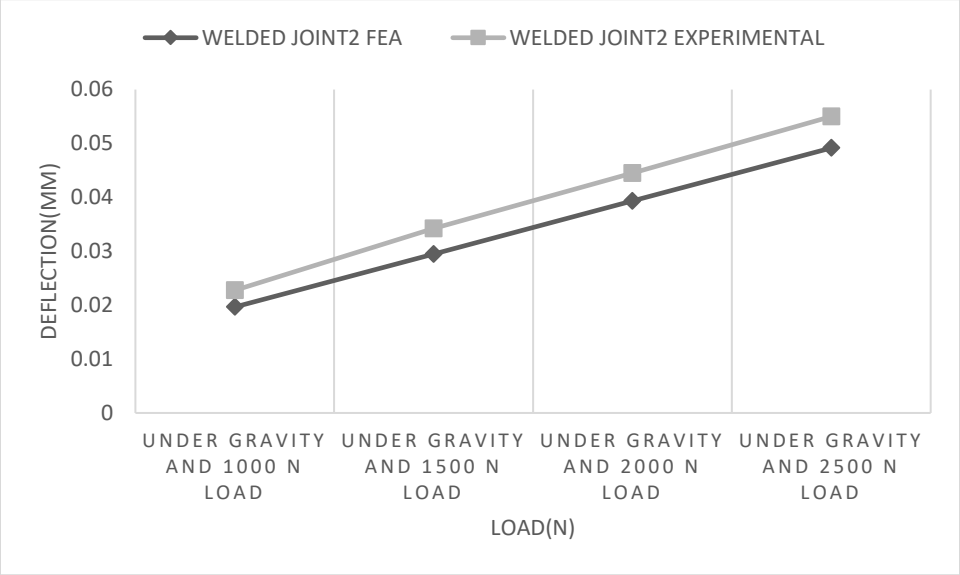

Figure 5.3: Graphical representation of welded Joint2 FEA and Experimental

Validation of all joint done by experimental and FEA and we found that maximum percentage difference 14.7% and minimum 10.54%. Now we can take the maximum percentage difference for further study. This percentage difference is later added because FEA results are less than comparing to experimental. The actual strength of the joints by FEA can possible only if we add percentage difference.

5.3 Validation of stand simulation using a measuring quantity deflection

Validation of a portable stand is possible by comparing experimental results with FEA results. base1 step1, base2 step2, seat1 step1 and seat2 step2 are validated and noted the percentage difference between them. This percentage difference helps us to find the actual strength of the base1 step1, base2 step2, base3 step3, base4 step4 and seat1 step1, seat2 step2, seat3 step3, seat4 step4.

Figure 5.4: Stand structure steps

5.3.1 Validation of Base1 Step1

Table 5.4 shows that the percentage difference between experimental and FEA results of Base1 Step1. Figure 5.5 shows that all experimental results greater than FEA results. Maximum value of percentage difference 20.3 and minimum is 15.5.

Table 5.4: Validation of base1 step1

Load (N)	Experimental (mm)	FEA (mm)	Percentage Difference
600	0.56	0.47	16.07
686.46	0.63	0.5315	15.5
1372.93	1.01	0.8446	16.4
2216.30	1.38	1.1219	18.7
3226.38	1.54	1.2263	20.3

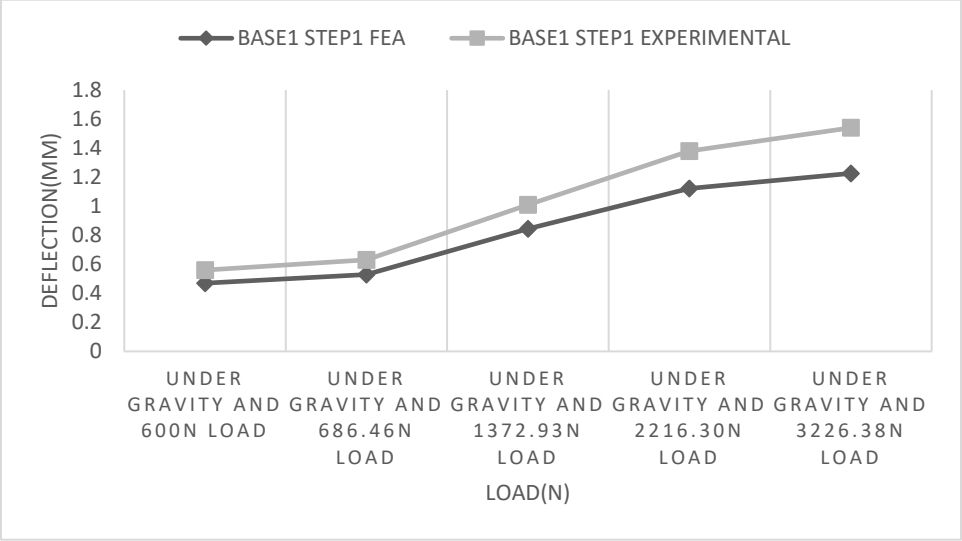

Figure 5.5: Graphical representation of base1 step1 FEA and Experimental

5.3.2 Validation of Base2 Step2

Table 5.5 shows that percentage difference between experimental and FEA results of Base2 Step2. Figure 5.6 shows that all experimental results greater than FEA results. Maximum value of percentage difference 17.29 and minimum is 12.

Table 5.5: Validation of base2 step2

Load (N)	Experimental (mm)	FEA (mm)	Percentage Difference
]600	0.7	0.58	17.14
686.46	0.75	0.66	12
1372.93	1.25	1.06	15.2
2216.30	1.69	1.428	15.5
3226.38	1.92	1.588	17.29

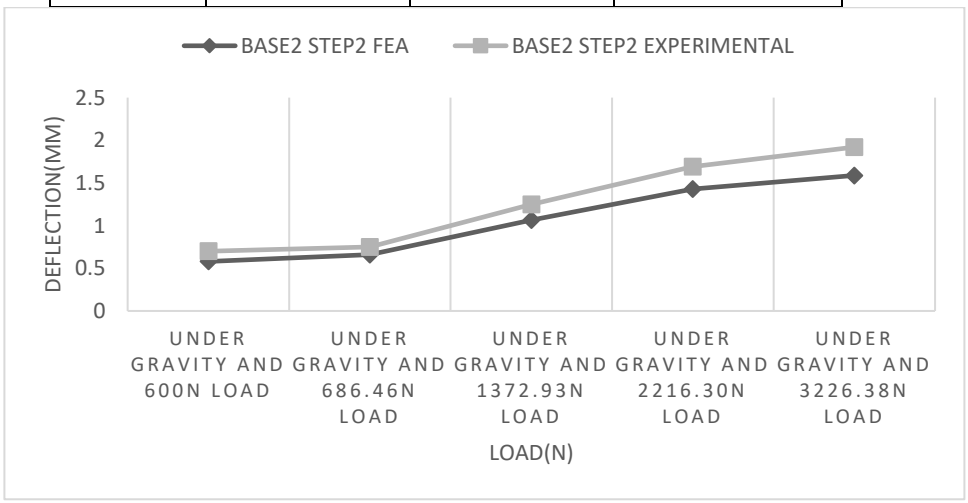

Figure 5.6: Graphical representation of base2 step2 FEA and Experimental

5.3.3 Validation of Seat1 Step1

Table 5.6 shows that the percentage difference between experimental and FEA results of Seat1 Step1. Figure 5.7 shows that all experimental results greater than FEA results. Maximum value of percentage difference 20.17 and minimum is 13.48.

Table 5.6: Validation of seat1 step1

Load (N)	Experimental (mm)	FEA (mm)	Percentage Difference
600	0.79	0.68	13.92
686.46	0.89	0.77	13.48
1374.86	1.41	1.16	17.73
2108.42	2.04	1.66	18.62
2804.7	2.31	1.844	20.17

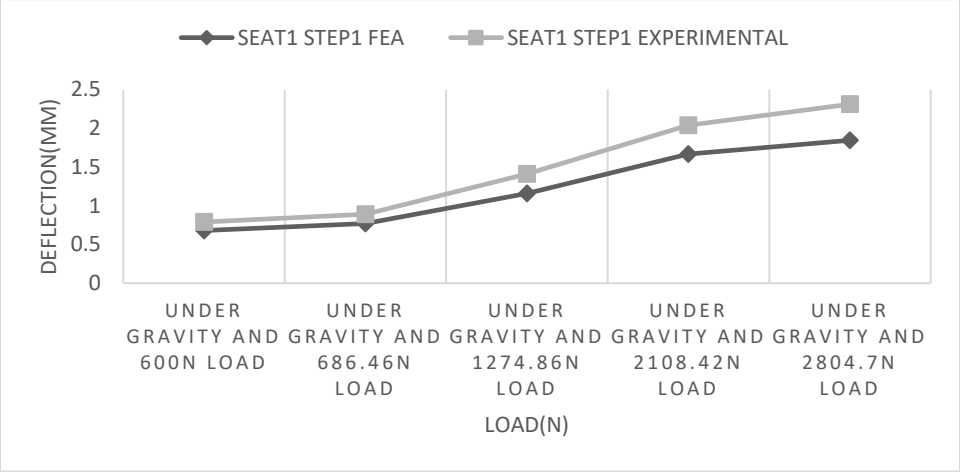

Figure 5.7: Graphical representation of seat1 step1 FEA and Experimental

5.3.4 Validation of Seat2 Step2

Table 5.7 shows that the percentage difference between experimental and FEA results of Seat2 Step2. Figure 5.8 shows that all experimental results greater than FEA results. Maximum value of percentage difference 19.1 and minimum is 10.92.

Table 5.7: Validation of seat2 step2

Load (N)	Experimental (mm)	FEA (mm)	Percentage Difference
600	0.76	0.677	10.92
686.46	0.86	0.76	11.6
1374.86	1.38	1.216	11.8
2108.42	2.01	1.648	18.0
2804.7	2.25	1.82	19.1

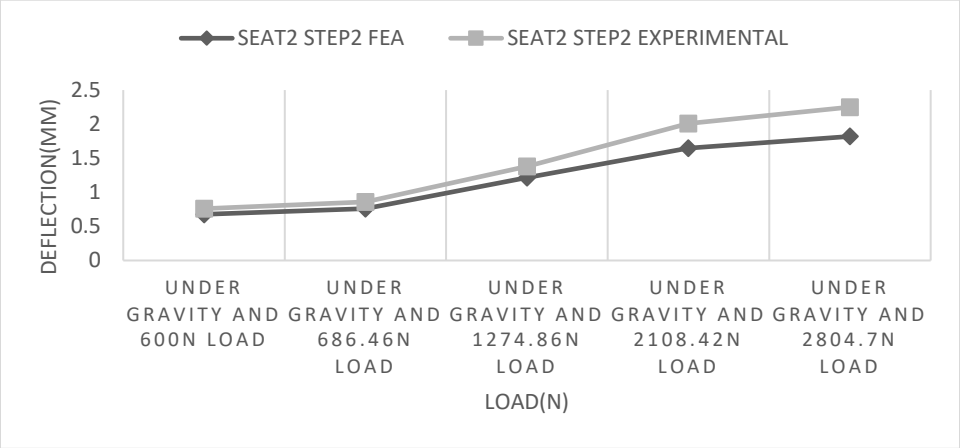

Figure 5.8: Graphical representation of seat2 step2 FEA and Experimental

Validation of stand done by experimental and FEA and we found that maximum percentage difference 20.17% and minimum 10.92%. Now we can take the maximum percentage difference for further study.

5.4 Experimental study only using simulation

- **Study of Base3 Step3 under static loading**

  Figure 5.9 shows a load of 3226.38 N which is applied at stand defined surface base3 step3. When a load of 3226.38 N is applied in presence of gravity, the resulting deflection and stress of the portable stand are shown in Figure 5.9(a) and Figure 5.9(b) respectively.

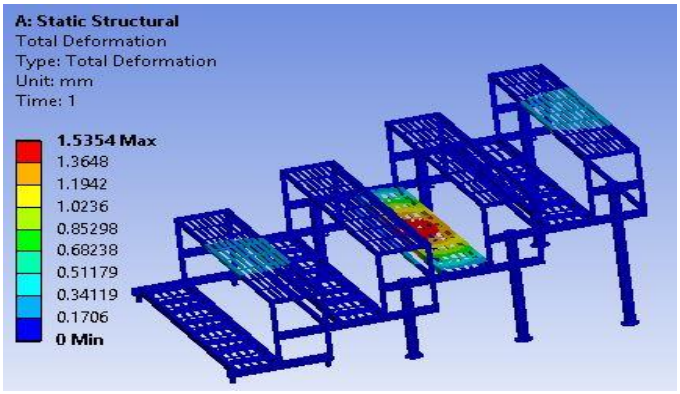

(a)

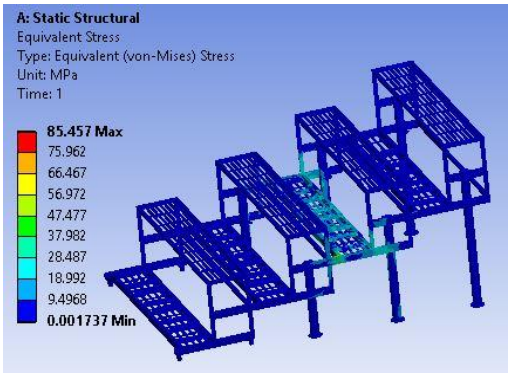

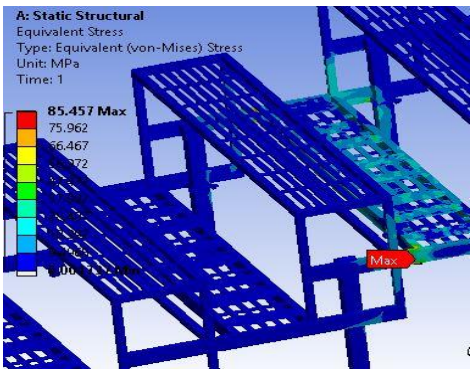

(b) (c)

Figure 5.9: Static loading for base3 step3 (a) Total deflection (b) Maximum stress (c) Zoomed view of maximum stress

Using the static force on base3 step3 Maximum stress and Total deflection is 85.45 MPa and 1.535 mm respectively.

- **Study of Base4 Step4 under static loading**

  Figure 5.10 shows a load of 3226.38 N which is applied at stand defined surface base4 step4. When a load of 3226.38 N is applied in presence of gravity, the resulting deflection and stress of the portable stand are shown in Figure 5.10(a) and Figure 5.10(b) respectively.

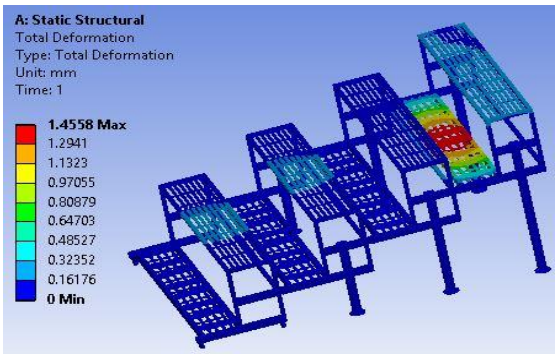

(a)

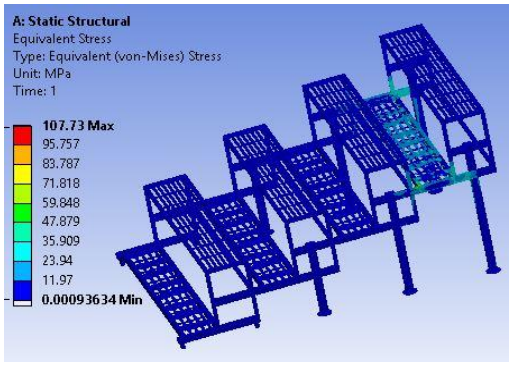

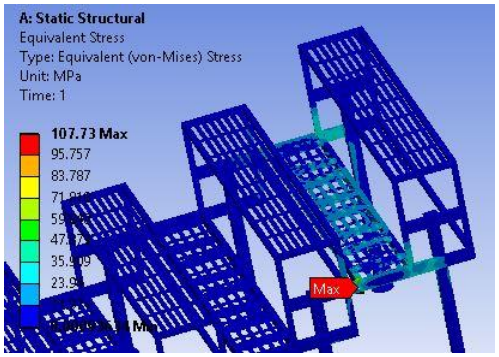

(b) (c)

Figure 5.10: Static loading for base4 step4 (a) Total deflection (b) Maximum stress (c) Zoomed view of maximum stress

Using the static force on base4 step4 Maximum stress and Total deflection is 107.73 MPa and 1.4558 mm respectively.

- **Study of all seats under static loading**

  Figure 5.11 shows when stand full with the audience and a load of 2804.7 N which is applied at stand defined surface. When a load of 2804.7 N is applied in presence of gravity, the resulting deflection and stress of the portable stand are shown in Figure 5.11(a) and Figure 5.11(b) respectively.

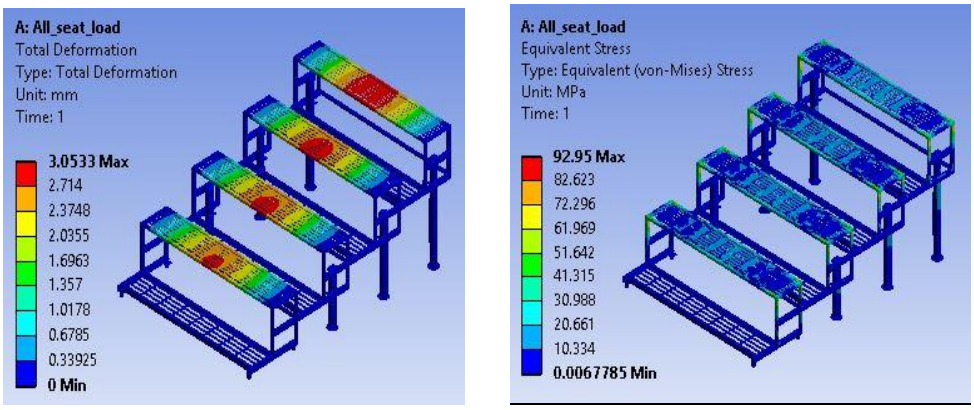

(a) (b)

Figure 5.11: Static loading for all seats (a) Total deflection (b) Maximum stress

Using the static force on all bases Maximum stress and Total deflection is 92.95 MPa and 3.053 mm respectively.

5.5 Impact loading

When the weight is applied at the middle of the beam, it tries to deflect the beam with respect to applied load. Different type of load applied to the stand and deflection is measured in dial indicator. Cross-check the deflection of Stand another instrument digital vernier height gauge used to measure the deflection of the stand. Vernier height gauge setup used in such a way that when the load is applied, it displaced and stop with respect to the deflection of the stand.

DMF is defined as the ratio of dynamic force over static force. The present work is to determine the static deflection for calculation of DMF. Due to this dynamic force can calculate. For this, it is necessary to carry-out static deflection calculations. At first, a static analysis of all mentioned loads is carried out. In the next step, calculation of DMF and with the help of DMF, dynamic force have calculated.

Figure 5.12: Stand structure with vernier height gauge

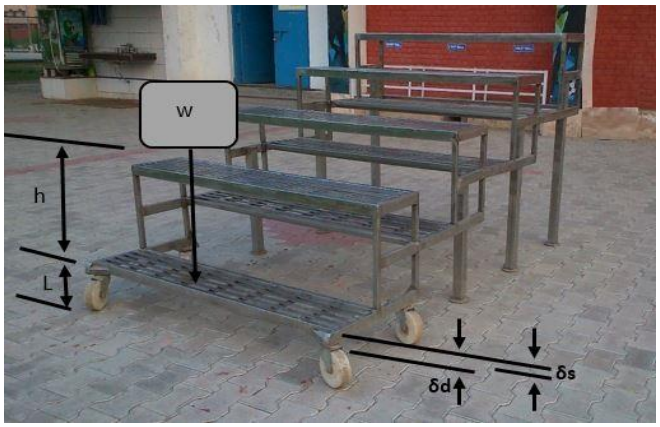

Figure 5.13: Impact loading for stand structure

h = 548.64 mm

The actual height of base1 step1 to seat1 step1 is 457.2 mm but we take assumption 20 % more as we consider a person jump 20% more for the given height.

For simply supported beam value of K, Appendix A.9

K = 219818.6

δ_S = static deflection

Static deflection already calculated for base1 step1 and base2 step2 for maximum load 3226.38N.

We know that from chapter three dynamics force analysis:

$$\mathrm{DMF} = 1 + \sqrt{1 + \frac{2h}{\delta_S}} \tag{5.1}$$

$$F_d = \mathrm{DMF} \times K \times \delta_s \tag{5.2}$$

5.5.1 Impact loading for base1 step1

For base1 step1 maximum static deflection 0.0012263 m at 3226.35 N load.

DMF = 30

$$F_d = 8086.908 \text{ N}$$

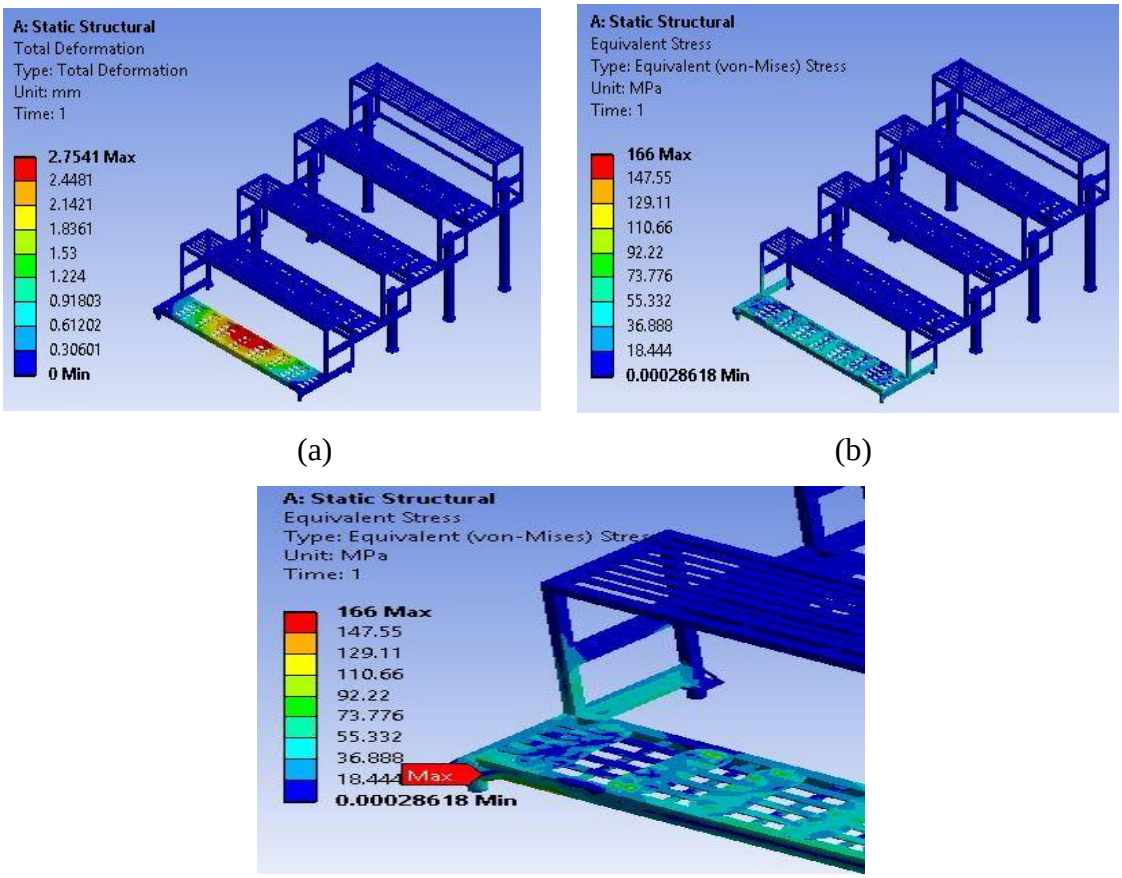

(a) (b)

(c)

Figure 5.14: Impact loading base1 step 1(a) Maximum deflection (b) Maximum stress (c) Zoomed view of maximum stress

Using the dynamic force on base1 step1 Maximum stress and Total deflection is 166 MPa and 2.75 mm respectively.

5.5.2 Impact loading for base2 step2

For base2 step2 maximum static deflection 0.001588 m at 3226.35 N load.

$$DMF = 27.37$$

$$F_d = 9554.09 \text{ N}$$

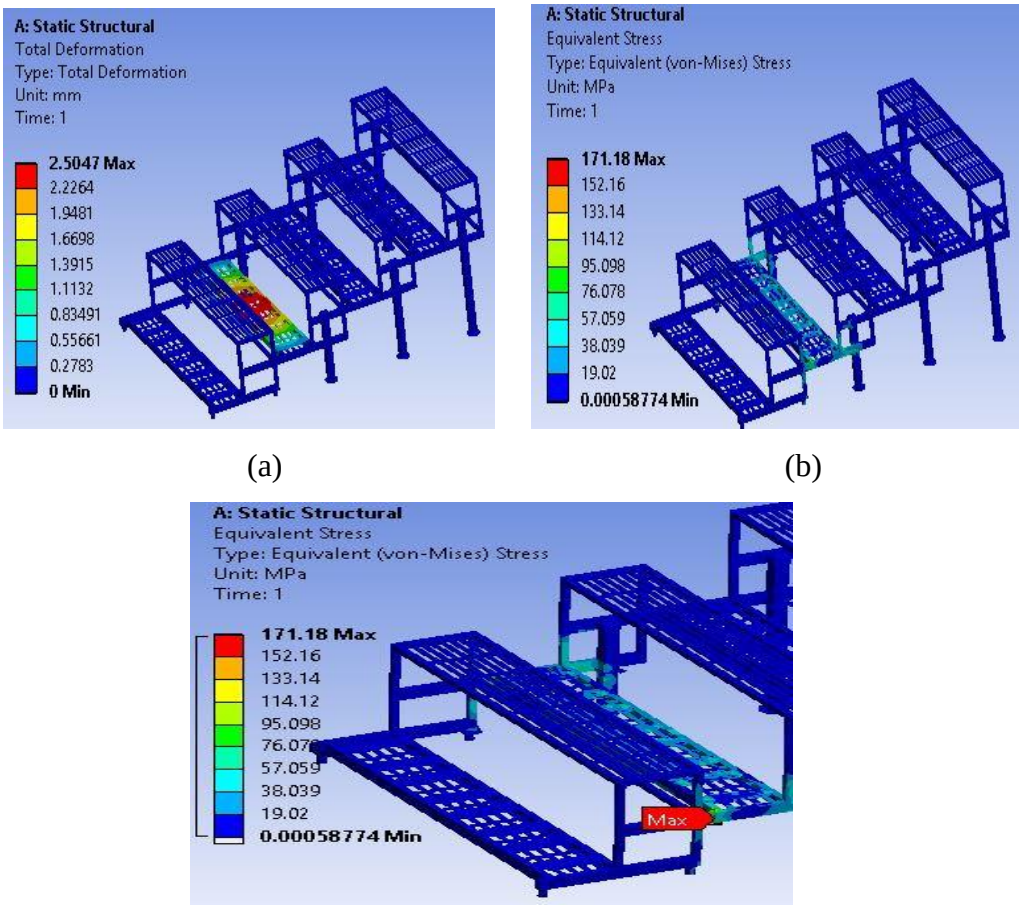

Figure 5.15: Impact loading base2 step2 (a) Maximum deflection (b) Maximum stress (c) Zoomed view of maximum stress

Using the dynamic force on base2 step2 Maximum stress and total deflection is 171.18 MPa and 2.50 mm respectively.

5.5.3 Impact loading for base3 step3

For base3 step3 maximum static deflection 0.001535 m at 3226.35 N load.

$$DMF = 27.7$$

$$F_d = 9346.57 \text{ N}$$

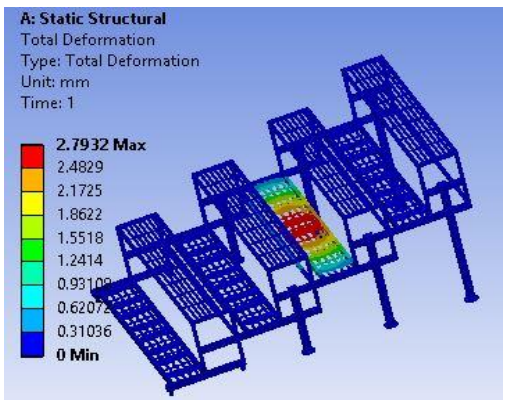

(a)

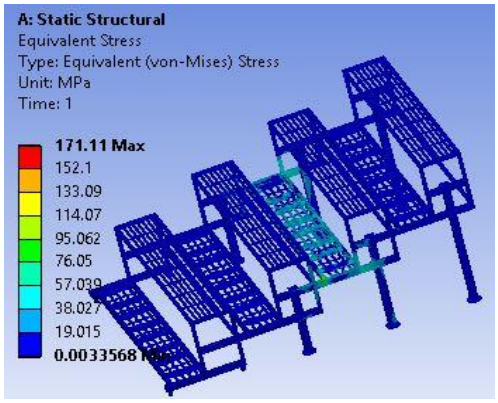

(b)

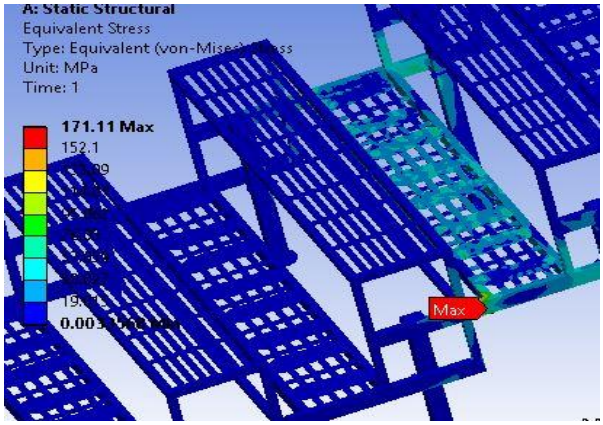

(c)

Figure 5.16: Impact loading base3 step3 (a) Maximum deflection (b) Maximum stress (c) Zoomed view of maximum stress

Using the dynamic force on base3 step3 Maximum stress and Total deflection is 171.11 MPa and 2.79 mm respectively.

5.5.4 Impact loading for base4 step4

For base4 step4 maximum static deflection 0.001455 m at 3226.35 N load.

$$DMF = 28.47$$

$$F_d = 9110.77 \text{ N}$$

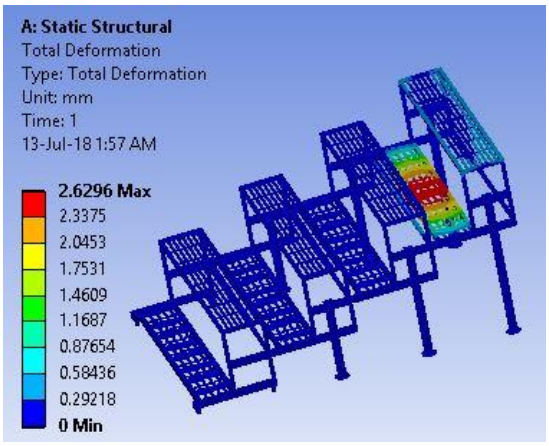

(a)

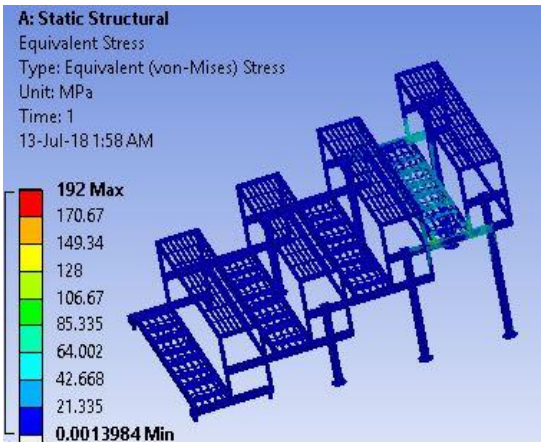

(b)

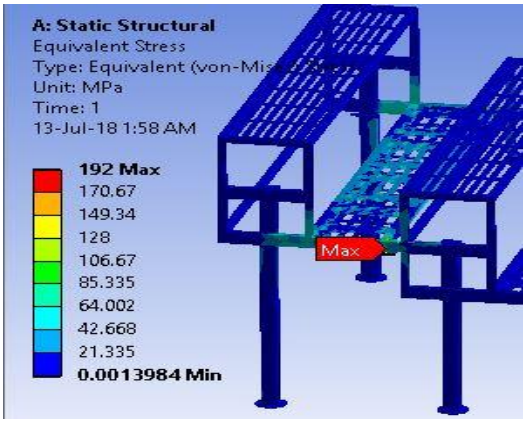

(c)

Figure 5.17: Impact loading base4 step4 (a) Maximum deflection (b) Maximum stress (c) Zoomed view of maximum stress

Using the dynamic force on base3 step3 Maximum stress and Total deflection is 192 MPa and 2.629 mm respectively.

5.5.5 Impact loading for all bases

When persons sitting on higher level seats that are seat1step1, seat2step2, seat3step3 and seat4step4 would step down or jump down to lower level base1step1, base2step2, base3step3 and base4step4 respectively in the process of vacating the stand the impact force for base1step1, base2step2, base3step3 and base4step4 can be calculated using all bases dynamics force.

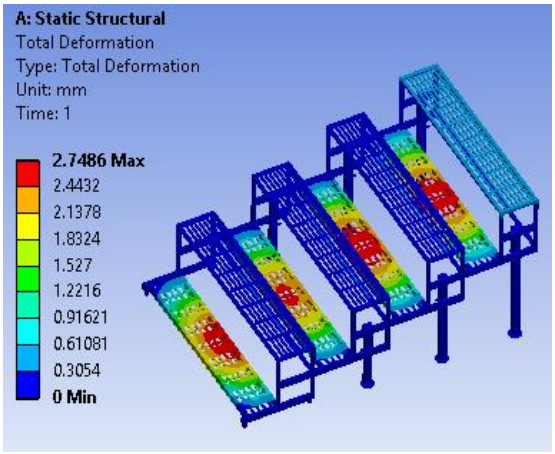

(a)

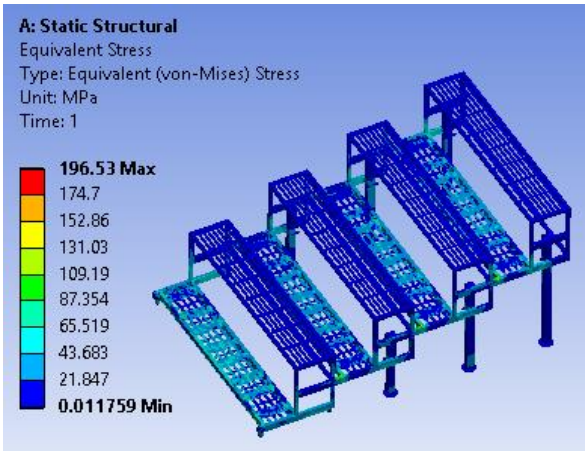

(b)

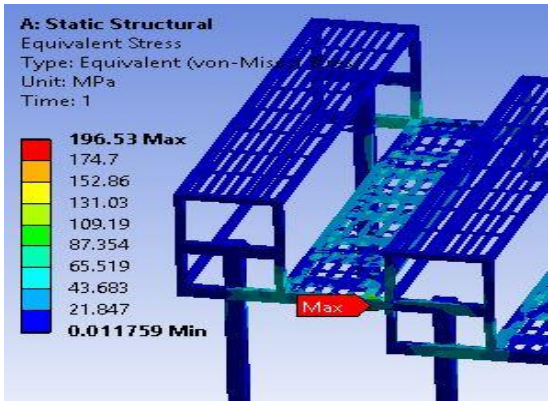

(c)

Figure 5.18: Impact loading all bases (a) Maximum deflection (b) Maximum stress (c) Zoomed view of maximum stress

Using the dynamic force on all bases Maximum stress and Total deflection is 196.53 MPa and 2.748 mm respectively.

5.6 Factor of safety

We can find the location of the maximum Von Misses stress of the folding stand which is shown in Figure 5.28. Based on the static safety factor theory, the formula for Factor of Safety (FOS) is defined by **[Case et al., 2013].**

$$\text{FOS} = \frac{\text{Significant strength of the material}}{\text{Corresponding significant stress from normal load}}$$

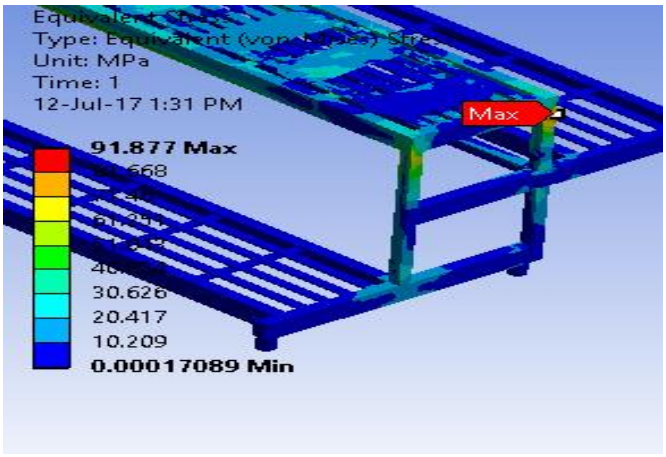

Figure 5.28: Maximum stress location

Welded joints FOS is affected by method and quality of weld design, shape, machining of weld surface and operation conditions. It is necessary to specify the factor of safety for the welded joint as weld breaking is a potential threat to human life. Joints tested for static loading and perceived that joint1 link1 and joint1 link2 are connected with each other so load divide between them and FOS increase. FOS for joints shown in Table 5.9.

Table 5.9: FOS for stand joints under static loading

	Load (N)	Stress (MPa)	Percentage Difference	FOS
Joint 1 Link1	2000	20.273	13.43	13.92
Welded Joint 1 Link 2	2000	159.5	13.86	1.77
Welded joint 2	2000	62.78	11.46	4.42

FOS for stand steps and when all audience sitting on it shown in Table 5.10.

Table 5.10: FOS for stand steps under static loading

	Load (N)	Stress (MPa)	Percentage Difference	FOS
Stand base1 step1	3226.38	71.565	20.3	3.47
Stand base2 step2	3226.38	83.87	17.29	2.65
Stand seat1 step1	2804.7	91.80	20.17	3.25
Stand seat2 step2	2804.7	90.209	19.1	3.28
Stand all seats	2804.7	92.95	20.0	3.20

Table 5.11 shows that the FOS of the stand bases under impact loading. In case of base1 step1 stress is 166 MPa but to validate this we need to add percentage difference. Actual FOS is 1.5. Then add 20.3 percent of 166 MPa. The calculated FOS result is 1.8.

Table 5.11: FOS for stand bases under impact loading

	Load(N)	Stress(MPa)	Percentage Difference	FOS
Stand base1 step1	3226.38	166.0	20.3	1.80
Stand base2 step2	3226.38	171.18	17.29	1.70
Stand base3 step3	3226.38	171.11	18.0	1.72
Stand base4 step4	3226.38	192.0	18.0	1.53
Stand all bases	3226.38	196.53	20.0	1.52

Portable stand impact loading results indicate that the factor of safety obtained from 1.52 to 1.80. If the worst case come and weight is more than the design limit. We have to redesign the stand bases to improve the FOS. Stand base and stand seats are analyzed using FEA for maximum loading and find that maximum stress appear at the welded joint 2 and seat legs. To improve the FOS of the portable stand we only analyzed these two because of maximum stress in it.

The value of factor of safety for various conditions of loading and material of structure recommends 1.5 to 2 for well-known material under reasonable environmental conditions **[Rahman et al., 2008].**

5.7 Redesign of the portable stand

Redesign of a stand structure possible by using FEA analysis. Using FEA we can find the maximum stress location of the structure and according to this, we can add material so we can reduce to stresses at a particular location. In stand structure, the material is added and also reduce rectangular beam so we can minimize stress and reduce the weight of structure respectively. Square Hollow section (SHS) 25.4 mm will be replaced by Rectangular Hollow section (RHS) 50.8 mm by 25.4 mm to decrease its stress. These are called legs of the seats.

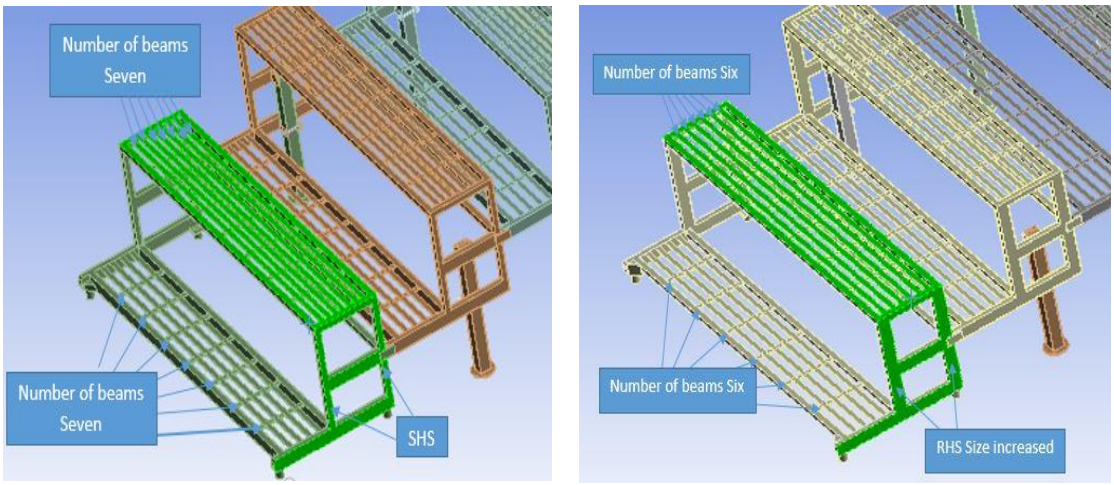

(a) (b)

Figure 5.19: Stand redesign (a) Actual stand cross-section (b) Redesigned stand cross section

- **Study of change in design parameter for Base1 Step1 under static loading**

  In base1 step1 we reduce the number of rectangular beams and does not add any material to the stand. Maximum stress and total deflection 74.411 MPa and 1.318 mm respectively. Due to reducing the number of rectangular beam total deflection and maximum stress increases but the weight of the structure decreases.

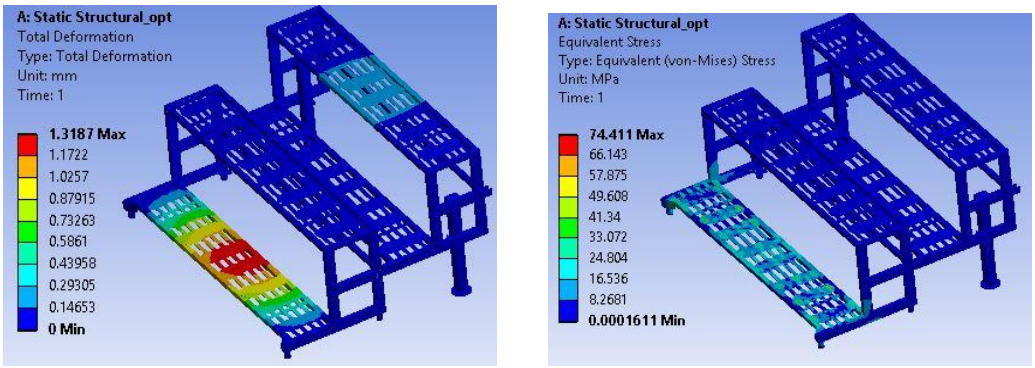

(a) (b)

Figure 5.20: Redesigned stand base1 step1 (a) Total deflection (b) Maximum stress

- **Study of change in design parameter for Base2 Step2 under static loading**

  In base2 step2 we reduce the number of rectangular beams and does not add any material in stand. Maximum stress and total deflection 85.909 MPa and 2.428 mm respectively.

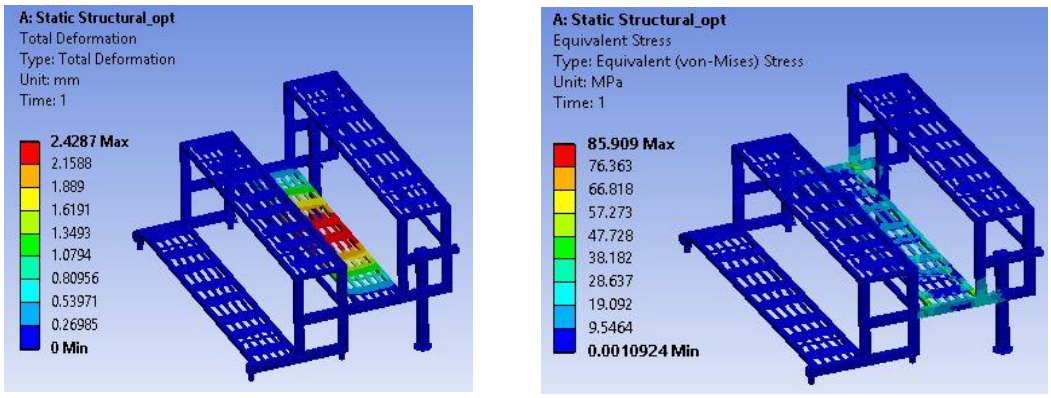

(a) (b)

Figure 5.21: Redesigned stand base2 step2 (a) Total deflection (b) Maximum stress

- **Study of change in design parameter for Seat1 Step1 under static loading**

  In seat1 step1 we reduce the number of rectangular beams and replace square hollow pipe 25.4 mm with rectangular pipe 25.4 mm by 50.8 mm and we observed that maximum stress reduce to 57.174 MPa.

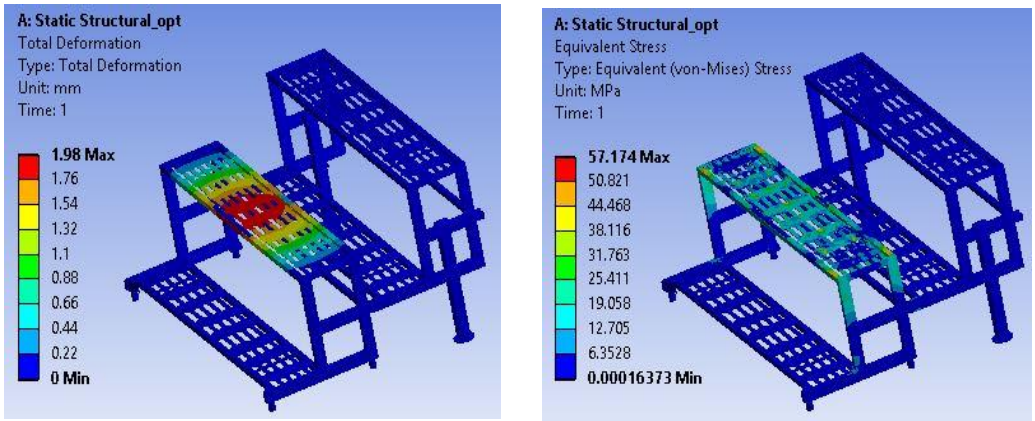

(a) (b)

Figure 5.22: Redesigned stand seat1 step1 (a) Total deflection (b) Maximum stress

- **Study of change in design parameter for Seat2 Step2 under static loading**

  In seat2 step2 we reduce the number of rectangular beams and replace square hollow pipe 25.4 mm with rectangular pipe 25.4 mm by 50.8mm and we observed that maximum stress reduce to 58.588 MPa.

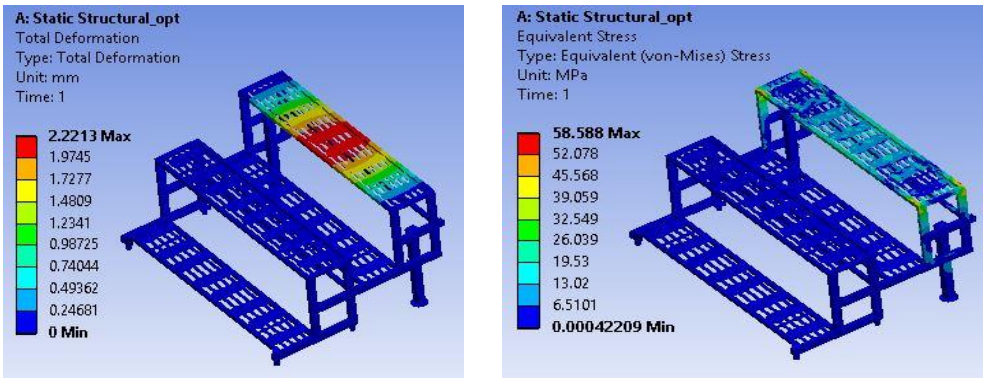

(a) (b)

Figure 5.23: Redesigned stand seat2 step2 (a) Total deflection (b) Maximum stress

- **Weight distribution**

  Deflection of the stand also depends upon weight distribution of the stand. Table 5.8 shows deflection with respect to the applied load. We observed that if weight distributed at center higher than sides then total deflection occurs at center more as compared to sides. If beam thickness increased, then the deflection of the portable stand can be reduced.

Table 5.8: Load distribution

Load (Kg)	Total load (N)	Deflection (mm)
140+110+120+130	4903.31	6.626
110+140+130+120	4903.31	7.2872

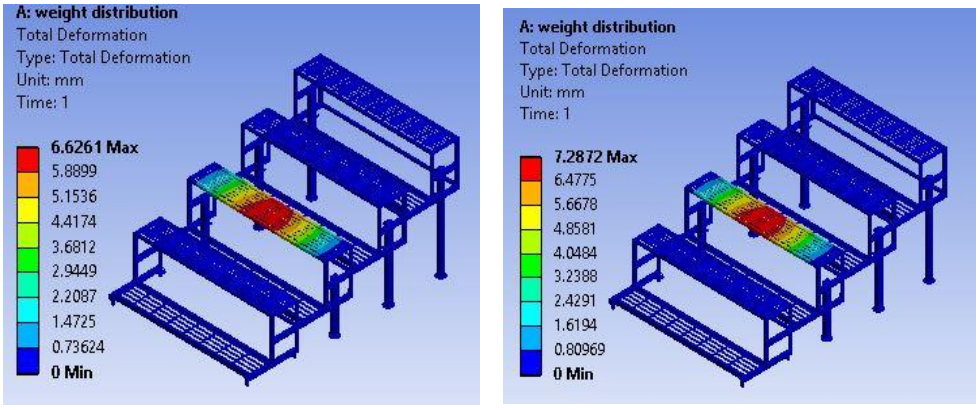

(a) (b)

Figure 5.24: Load distribution (a) maximum load at sides (b) maximum load at center

- **Thickness of the beam used in stand**

  For all experiments thickness 1.5 mm used but here we reduce the thickness of the stand to 1 mm and see deflection and stress of stand.

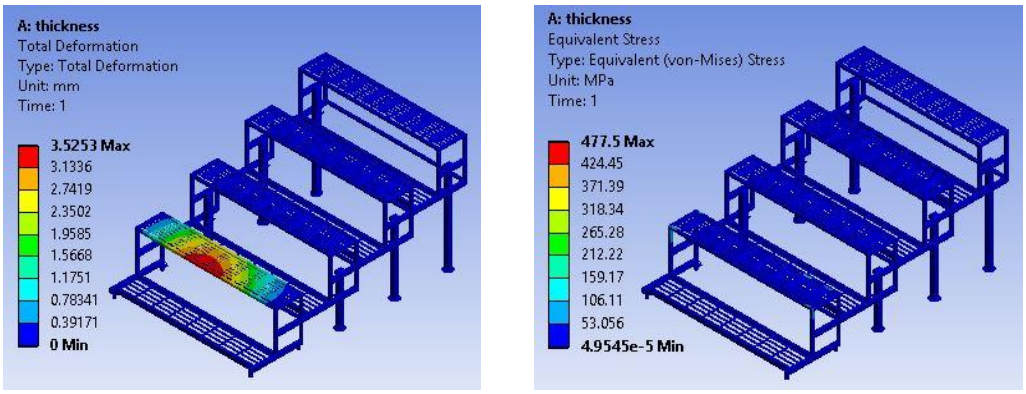

(a) (b)

Figure 5.25: Stand beam thickness analysis (a) maximum deflection (b) maximum stress

Seat1 Step1 loading under 1 mm thickness shown in Figure 5.25. Using static force 2804.7N on seat1 step1 Maximum stress and Total deflection is 477.5 MPa and 3.525 mm respectively. We conclude that 1mm thickness not safe for the stand. Either we use 1.5 mm or higher than that.

- **Add Grooves in the stand for lifting**

  The portable collapsible stand can be stored remotely and installed quickly on occasions when events are staged but for this, it is important to a portable stand can collapse easily with a lesser man and without any harm. We need to add groove here as there are very much higher chances that the fingers of the person can crush while collapsing the stand. It helps when finger inside while lifting.

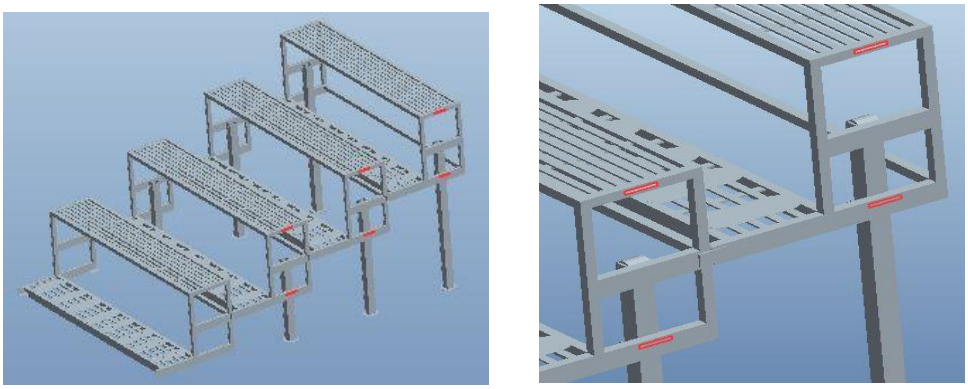

(a) (b)

Figure 5.26: Stand grooves (a) stand groove location (b) Zoomed view of a groove

- **Study of change in design parameter for welded joint 2**

  When we analyzed the stand bases with respect to applied load for static and dynamic, always maximum stress occurs at welded joint2. Due to impact load stand structure can fail so we need to increase the strength of the joint. Welded joint2 length (L) increases 30 mm to 40 mm and thickness also increases 5 mm to 8 mm. Maximum stress and total deflection of welded joint at 2000 N load 48.899 MPa and 0.0333 mm respectively.

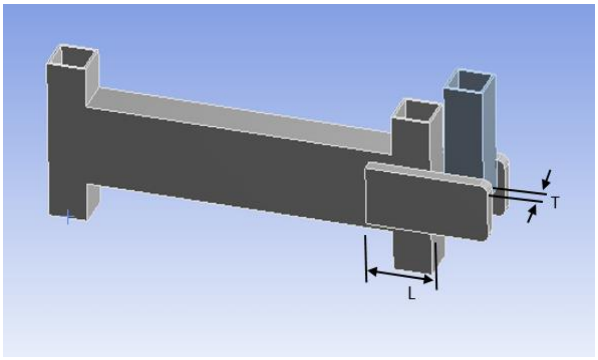

(a)

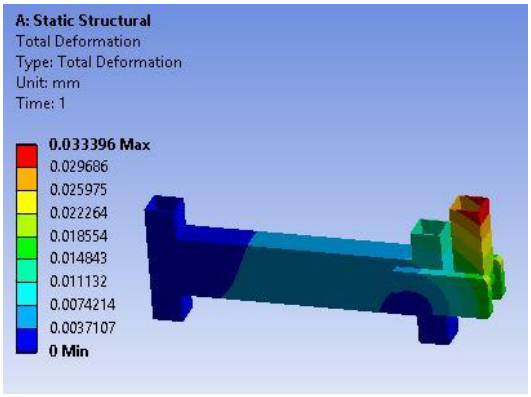

(b)

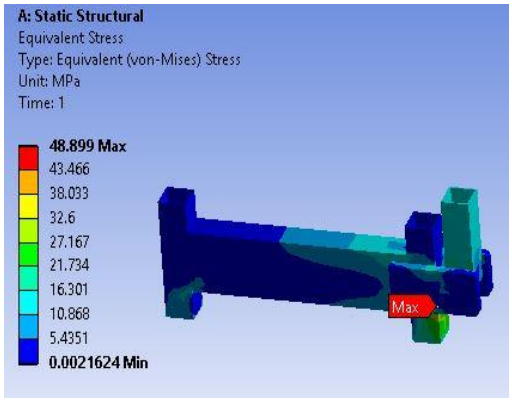

(c)

Figure 5.27: Redesigned welded joint 2 (a) joint geometry (b) total deflection (c) maximum stress

Table 5.12: FOS for the redesigned portable stand and joint under static loading

	Load (N)	Stress (MPa)	Percentage Difference	FOS	FOS Redesign
Stand base1 step1	3226.38	74.411	20.3	3.47	4.02
Stand base2 step2	3226.38	85.90	17.29	2.65	3.39
Stand seat1 step1	2804.7	57.174	20.17	3.25	5.23
Stand seat2 step2	2804.7	58.588	19.1	3.28	5.06
Welded joint2	2000	48.89	11.46	4.42	5.67

Weight of the portable stand is calculated using a Creo software. We observed that redesigned stand less weight as compare to the actual stand also FOS of the redesigned stand is greater than actual stand.

Table 5.13: Weight percentage difference between actual and redesigned stand

	Actual stand weight (kg)	Redesigned stand weight (kg)	Percentage difference
Actual stand weight	208	189	10.05

5.8 Welding defects

We observed that arc welding create cracks or even damage to stainless steel 202 product after some time with contact with moisture. Mostly welding affects the heat affected zone where welding takes place due to change in properties of the material.

Table 5.14: Defects due to welding

AISI 202 SS has similar mechanical properties as compared to AISI 304 SS grade. But the ability to resist corrosion is somewhat less as compare to AISI 304 SS so it is used for indoor applications **[Bharwal and Vyas, 2014]**. Due to less resist corrosion and stand used for outdoor applications corrosion takes place mostly welded part of the stand and cause cracks and broken.

Chapter 6

Conclusions and Scope for Future Work

6.1 Conclusion

- Deflection on the welded joint1 link2 is more as compare to joint1 link1 and welded joint2. It is because of joint design and load distribution.
- Factor of Safety is more at joint1 link1 as compare to joint1 link2 and welded joint2 for static loading.
- Portable stand impact loading results indicate that the factor of safety obtained from 1.52 to 1.80. If the worst case come i.e. weight is more than the design limit. We have to redesign the stand bases to improve the FOS.
- FEA results show that 1 mm thickness of the stand beam not feasible as stress increases more than yield strength. We can use a 1.5 mm thickness of the beam or more than that to increase the FOS.
- Stand base is analyzed using FEA for maximum loading and find that maximum stress appear at the welded joint 2.
- Stand seat is analyzed using FEA for maximum loading and identify that maximum stress appear at the seat legs.
- The weight of the portable stand is reduced by reducing the rectangular beams from the stand bases and seats.
- When we redesign the welded joint2 and stand seat legs then FOS of stand bases and stand seats increased.
- Overall weight of the redesigned portable stand decreased and it helps during transportability.

6.2 Scope for the future work

There is a number of different parameters which are well suited for an analysis for stand frame but due to the complexity of the stand frame, only some parameter has been chosen. However, there are further studies that can be made in order to investigate a Stand frame. Some of these further studies are listed below:

- Study of the welding processes for Stainless Steel 202 can be possible. It may increase the strength of the stand and its joints.

- Strength of the stand frame is very much depending on the stand joints so different possible way which can be considered fabricating stand joints. This will have a great impact on the strength of the stand frame.
- The cross-section of the stand frame could be studied further for different cross-section so it would help us in less deflection.

References

[1] A. Miyoshi, G. Yagawa, and S. Sasaki, “An interface agent that actively supports CAE beginner users in performing analyses,” vol. 30, pp. 575–579, 1999.

[2] N. S. Kuralay, “Stress analysis of a truck chassis with riveted joints,” vol. 38, pp. 1115–1130, 2002.

[3] D. roger west and D. vikram Pakrashi, “Designing against Structural Failure,” pp. 1-5, 2007.

[4] N. Ye and T. Moan, “International Journalof Fatigue Static and fatigue analysis of three types of aluminium box-stiffener / web frame connections,” vol. 29, pp. 1426–1433, 2007.

[5] E. Wang and R. Rauch, “2008 International ANSYS Conference Fatigue analysis and design optimization of a trailer hitch system,” pp. 1–32, 2008.

[6] K. Krishan, “Establishing correlation of footprints with body weight — Forensic aspects,” vol. 179, pp. 63–69, 2008.

[7] R. A. Rahman, M. N. Tamin, O. Kurdi, and J. Bahru, “Stress Analysis of heavy duty truck chassis as a preliminary data for its fatigue life prediction using FEM,” no. 26, pp. 76–85, 2008.

[8] C. Liu, X. Liu, and H. Huang, “Simulation Research on Structural Strength of The Hub Plate,” pp. 1310–1312, 2009.

[9] M. M. Topaç, H. Günal, and N. S. Kuralay, “Fatigue failure prediction of a rear axle housing prototype by using finite element analysis,” *Eng. Fail. Anal.*, vol. 16, no. 5, pp. 1474–1482, 2009.

[10] G. Xu and B. R. Ellingwood, “Disproportionate collapse performance of partially restrained steel frames with bolted T-stub connections,” *Eng. Struct.*, vol. 33, no. 1, pp. 32–43, 2011.

[11] G. Salvendy, *Handbook of human factors and ergonomics*. John Wiley & Sons ISBN: 978-1-118-13149-7, 2012.

[12] M. Azizi, M. Nor, H. Rashid, W. Mohd, and F. Wan, “Stress Analysis of a Low Loader Chassis,” vol. 41, no. Iris, pp. 995–1001, 2012.

[13] A. H. Case, John and Chilver, “Strength of materials and structures,” John Wiley & Sons, ISBN 0 470 37980 4, pp. 706, 2013.

[14] A. Singh, V. Soni, and A. Singh, “Structural Analysis of Ladder Chassis for Higher Strength,” vol. 4, no. 2, pp. 253–259, 2014.

[15] V. K. Sharma and M. Kainth, “Effect of Auxiliary Mechanical Vibrations on Mechanical and Metallurgical properties of Stainless,” vol. 1, no. 1, pp. 1–6, 2014.

[16] S. Li, Z. Guo, S. Cheng, and X. Zhang, “Design optimization of sheet metal stamped parts by CAE simulation and back-propagation neural network,” *Procedia Eng.*, vol. 81, no. October, pp. 1023–1028, 2014.

[17] S. Bharwal and C. Vyas, “Weldability Issue of AISI 202 SS (Stainless Steel) Grade with GTAW Process Compared to AISI 304 SS Grade,” vol. 4, no. 6, pp. 695–700, 2014.

[18] M. Pavlović, C. Heistermann, M. Veljković, D. Pak, M. Feldmann, C. Rebelo, and L. Simões da Silva, “Friction connection vs. ring flange connection in steel towers for wind converters,” *Eng. Struct.*, vol. 98, pp. 151–162, 2015.

[19] M. Hill, R. Naemi, H. Branthwaite, and N. Chockalingam, “The relationship between arch height and foot length : Implications for size grading,” *Appl. Ergon.*, vol. 59, pp. 243–250, 2017.

Appendix

A.1 Bend test graph results for AISI 202

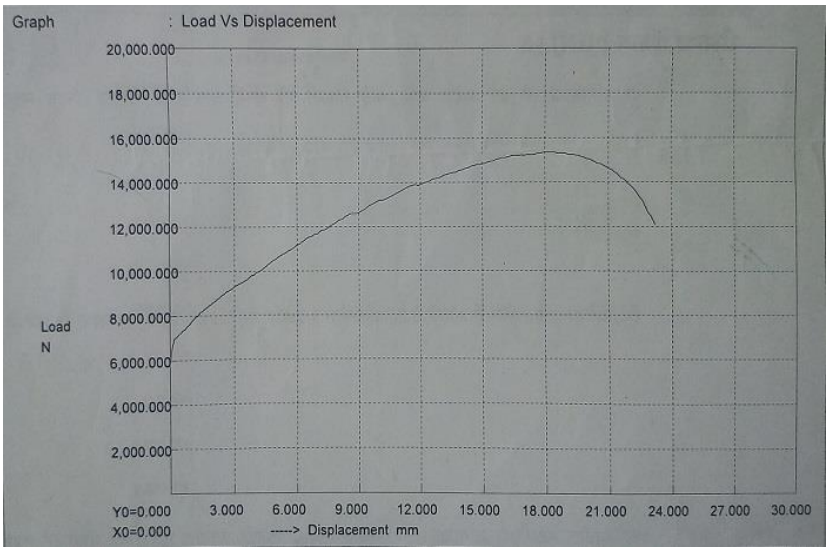

Figure A1.1: Graphical representation for Load vs Deflection for Experiment1

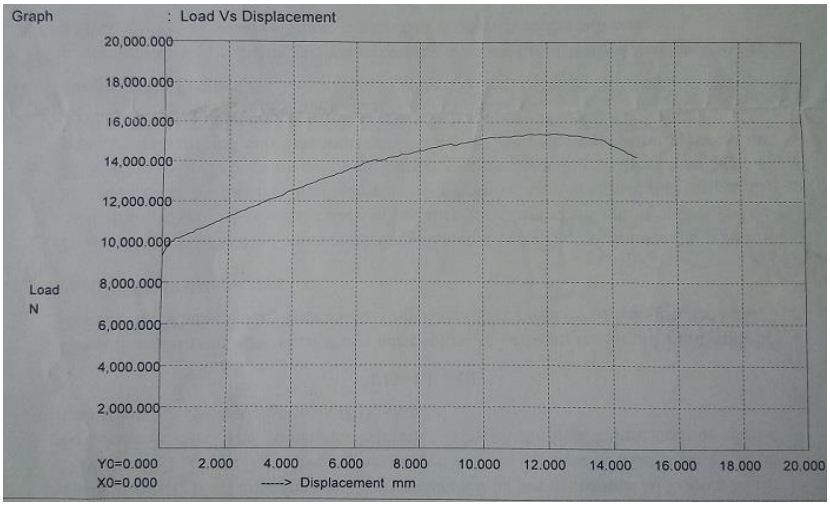

Figure A1.2: Graphical representation for Load vs Deflection for Experiment2

A.2 Measurement of Joint1 Link1

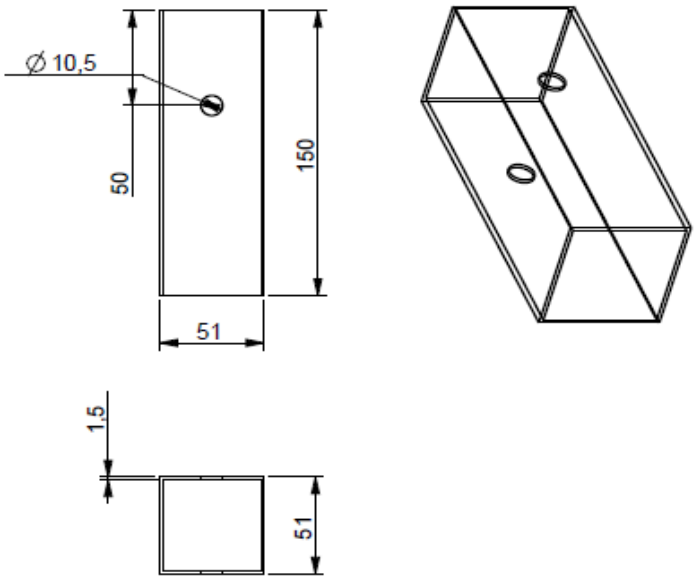

Table A2.1: Experimental values for joint1 link1

Load (N)	Experiment 1	Experiment 2	Experiment 3	Experiment4	Mean
1000	0.0032	0.0034	0.0031	0.0038	0.0034
1500	0.0048	0.0050	0.0052	0.0055	0.0051
2000	0.0063	0.0070	0.0066	0.0071	0.0067
2500	0.0080	0.0086	0.0084	0.0088	0.0084

A.3 Measurement of welded Joint1 Link2

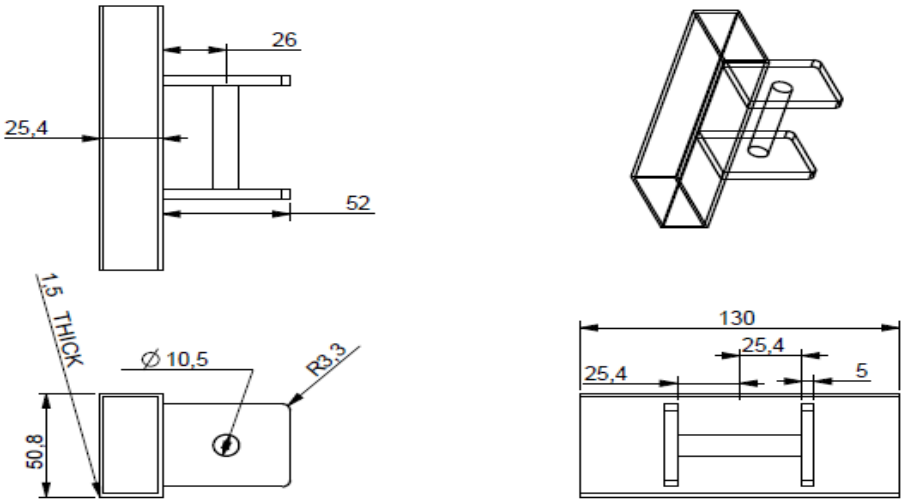

Table A3.1: Experimental values for welded joint1 link2

Load (N)	Experiment 1	Experiment 2	Experiment 3	Experiment4	Mean
1000	0.087	0.079	0.085	0.090	0.085
1500	0.120	0.126	0.130	0.124	0.125
2000	0.170	0.163	0.174	0.165	0.168
2500	0.207	0.222	0.219	0.216	0.216

A.4 Measurement of welded Joint2

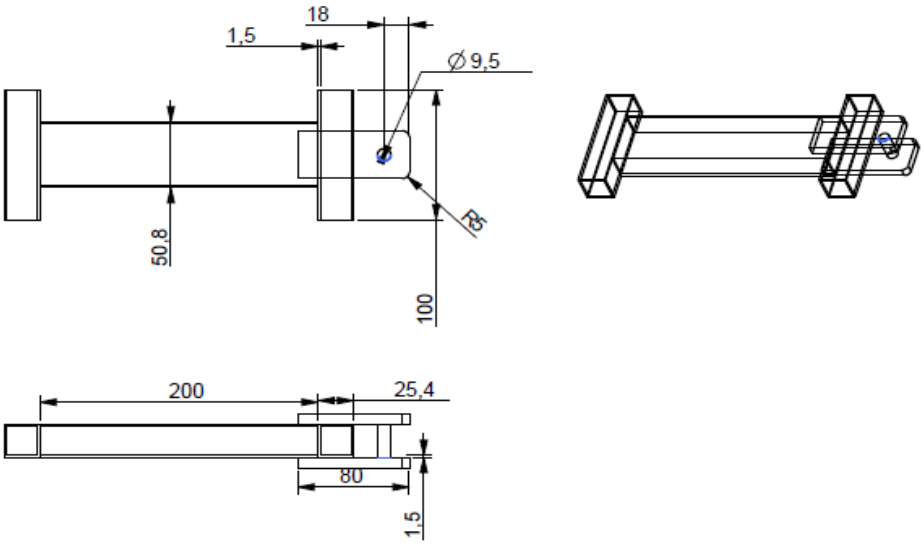

TableA 4.1: Experimental values for welded joint2

Load (N)	Experiment 1	Experiment 2	Experiment 3	Experiment4	Mean
1000	0.020	0.022	0.026	0.023	0.0227
1500	0.030	0.038	0.033	0.036	0.0343
2000	0.041	0.046	0.043	0.048	0.0445
2500	0.051	0.054	0.059	0.056	0.055

A.5 Measurement of foldable bench

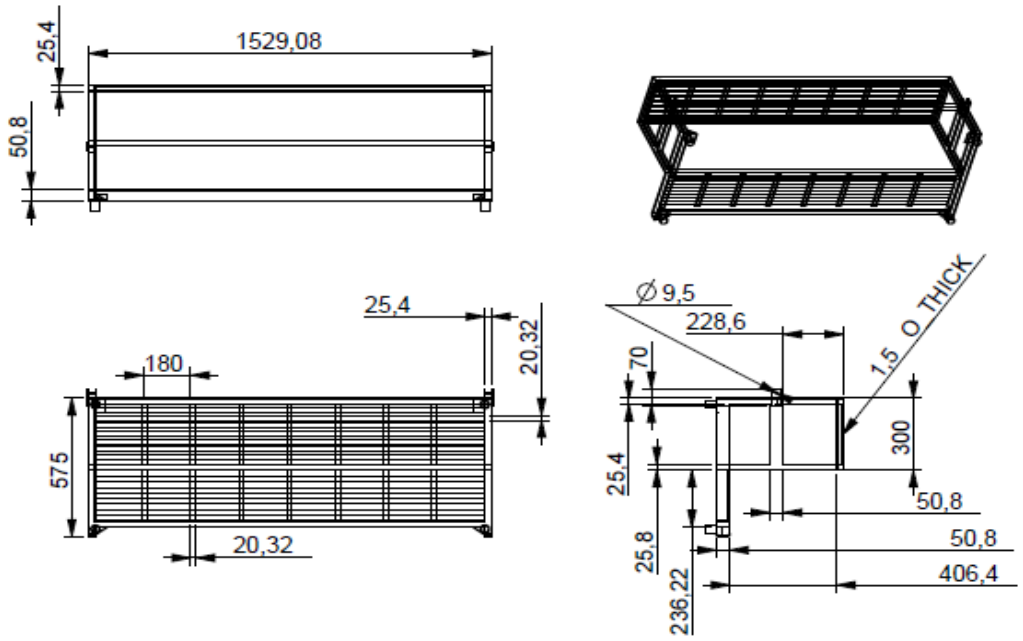

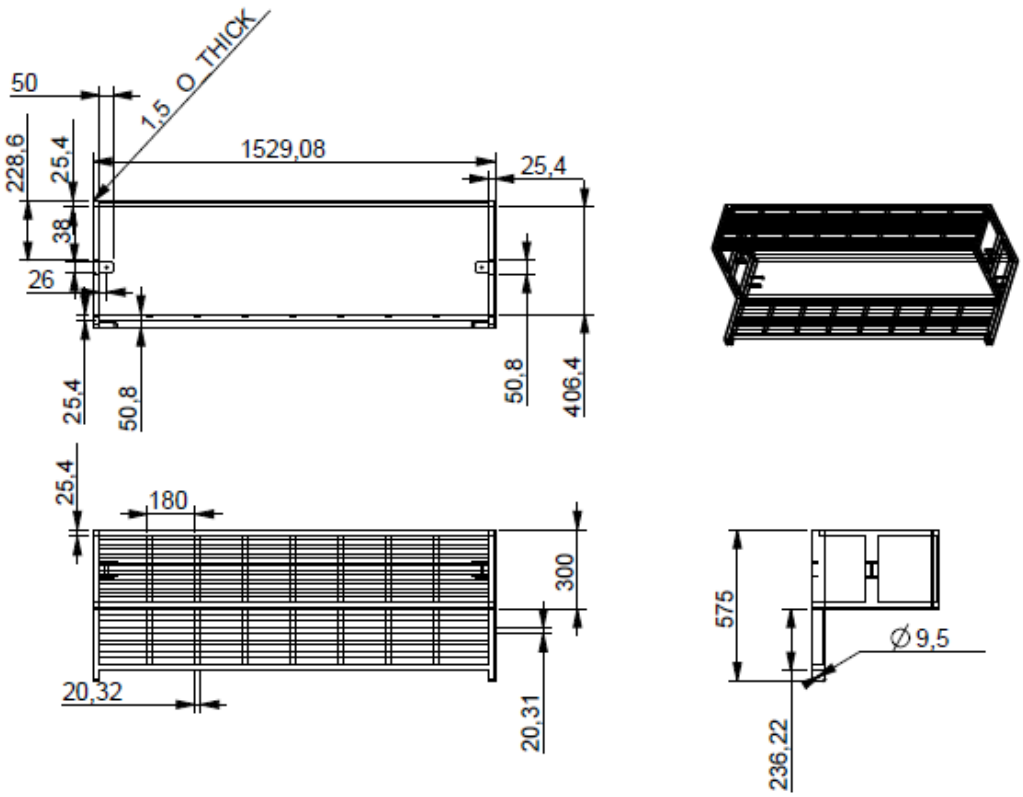

A.6 Dynamics Magnification Factor

h = Height of dropped weight

w = Dropped weight

δ_s = Static deflection of the structure under the weight

δ_d = Dynamic deflection

K = Stiffness of the distributed mass system of the bench

F_s =Static force

F_d = Dynamic force

For static loading

From Hooke's law:

$$F_s \alpha \delta_s$$

$$F_s = K\delta_s$$

$$F_s = m\,g$$

For dynamic loading

$$F_d \alpha \delta_d$$

$$F_d = K\delta_d$$

Dynamic force always greater than static force because of impact

$$\delta_s < \delta_d$$

Dynamics Magnification Factor (DMF):

$$DMF = \frac{F_d}{F_s} = \frac{\delta_d}{\delta_s}$$

Energy stored on bench:

From Hooke's law

$$F_s = Kx$$

x = deflection

$$F_s = mg$$

$$W = K\int_0^{\delta} x\,dx = \frac{K\delta^2}{2}$$

Apply Energy method:

Energy method is easy to extend to impact on a structure by a dropped mass. In this case the additional work done by the weight plus energy to be absorbed in the incoming kinetic energy.

$$E_{Initial} = E_{Final}$$

$$mg(h + L) = mg(L - \delta_d) + \frac{1}{2}K\delta_d^2$$

$$\frac{2h}{\delta_s} = -2\frac{\delta_d}{\delta_s} + \frac{\delta_d^2}{\delta_s^2}$$

$$(DMF)^2 - 2(DMF) - \frac{2h}{\delta_s} = 0$$

$$DMF = 1 + \sqrt{1 + \frac{2h}{\delta_S}}$$

Dynamics Magnification Factor with respect to dropped height and static deflection is shown in this equation. We can predict that from this equation as static deflection increases DMF decreases.

If h=0

$$\text{DMF} = \frac{F_d}{F_s} = 2$$

It means dynamics force is two times of static force.

If we know the velocity of mass then:

Equating kinetic energy on impact with potential energy on dropping from a height (h) that is:

$$mgh = \frac{mV^2}{2}$$

$$h = \frac{V^2}{2g}$$

$$\text{DMF} = 1 + \sqrt{1 + \frac{V^2}{g\delta_S}}$$

$$\text{DMF} = \frac{\sigma_d}{\sigma_s} = 1 + \sqrt{1 + \frac{V^2}{g\delta_S}}$$

Dynamics Magnification Factor with respect to velocity and static deflection is shown in this equation.

For dynamic force:

$$F_d = \text{DMF x } F_s$$

$$F_s = K\delta_s$$

$$F_d = \text{DMF x K x } \delta_s$$

A.7 Buckling analysis

When a straight column subjected to axial compression suddenly undergoes bending.

Critical buckling load P_{cr} for columns is theoretically given as

$$P_{cr} = \frac{\pi^2 EI}{(KL)^2}$$

Where, I = moment of inertia about the axis of buckling

K = effective length factor based on end boundary conditions

If one end fixed and other end pin joined then K = 0.7.

Square Hollow Section (SHS) used here with 50.8 mm wide by 50.8 mm high by 1.5 mm thick and length 1000 mm.

B = 0.0508 m, H = 0.0508 m

b = 0.0478 m, h = 0.0478 m

Moment of Inertia for square hollow section about X-X axis,

$$I = \frac{BH^3}{12} - \frac{bh^3}{12}$$

$$I = \left(\frac{0.0508 \text{ x } 0.0508^3}{12} - \frac{0.0478 \text{ x } 0.0478^3}{12}\right)$$

$I = 1.199\ x\ 10^{-7}\ m^4$

$$P_{cr} = \frac{\pi^2 EI}{(KL)^2}$$

$$P_{cr} = \frac{\pi^2 \text{ x } 210 \text{ x } 10^9\ x\ 1.199\ x\ 10^{17}}{(0.7 \text{ x } 1)^2}$$

$$P_{cr} = 506.64 \text{ KN}$$

$$\text{Safety Compressive Load} = \frac{\text{Buckling load}}{\text{Factor of safety}}$$

$$\text{Safety Compressive Load} = \frac{506.64}{3}$$

$$\text{Safety Compressive Load} = 168.88 \text{ KN}$$

A.8 Beam analysis

A rectangular hollow section type of beam used while fabricated the foldable bench. It's dimensions 50.8 mm by 25.4 mm with 1.5 mm thickness and length 1.5 m.

$$I = \frac{BH^3}{12} - \frac{bh^3}{12}$$

B = 0.0254 m, H = 0.0508 m

b = 0.0224 m, h = 0.0478 m

$$I = \left(\frac{0.0254 \text{ x } 0.0508^3}{12} - \frac{0.0224 \text{ x } 0.0478^3}{12}\right)$$

$I = 7.36\ x\ 10^{-8}\ m^4$

Consider a simply supported beam i.e. fixed at both ends and point load applied on the center then maximum deflection given as **[Case et al., 2013].**

$\delta_{max} =$ maximum deflection

$$\delta_{max} = \frac{WL^3}{48EI}$$

$$\delta_{max} = \left(\frac{600 \text{ x } 1.5^3}{48 \text{ x } 210 \text{ x } 10^9 \text{ x } 7.36 \text{ x } 10^{-8}}\right) \text{ x } 10^3$$

$\delta_{max} = 2.72$ mm

A.9 Stiffness of the rectangular hollow beam

In case of the simply supported beam, K is given by **[Case et al., 2013]**

$$K = \frac{48EI}{L^3}$$

$$K = \frac{48\ x\ 210\ x\ \ 10^9\ x\ 7.36\ x\ 10^{-8}}{1.5^3}$$

K = 219818.6

Dynamic force for Stand:

$$F_d = DMF \text{ x } K \text{ x } \delta_s$$

- Dynamic force for base1 step1

  For base1 step1 maximum deflection 0.0012263 m at 3226.35 N load and calculated DMF 30.

$$F_d = 30 \text{ x } 219818.6 \text{ x } 0.0012263$$

$$F_d = 8086.908 \text{ N}$$

- Dynamic force for base2 step2

  For base2 step2 maximum deflection 0.001588 m at 3226.35 N load and calculated DMF 27.37.

$$F_d = 27.37 \text{ x } 219818.6 \text{ x} 0.001588$$

$$F_d = 9554.09 \text{ N}$$

- Dynamic force for base3 step3

  For base3 step3 maximum deflection 0.001535 m at 3226.35 N load and calculated DMF 27.7.

$$F_d = 27.7 \text{ x } 219818.6 \text{ x } 0.001535$$

$$F_d = 9346.57 \text{ N}$$

- Dynamic force for base4 step4

  For base3 step3 maximum deflection 0.0014558 m at 3226.35 N load and calculated DMF 28.47.

$$F_d = 28.47 \text{ x } 219818.6 \text{ x } 0.0014558$$

$$F_d = 9110.78 \text{ N}$$

Navdeep Theis

ORIGINALITY REPORT

10%	8%	3%	5%
SIMILARITY INDEX	INTERNET SOURCES	PUBLICATIONS	STUDENT PAPERS

PRIMARY SOURCES

1	Submitted to National Institute of Technology, Rourkela Student Paper	1%
2	www.ap-printing.com Internet Source	1%
3	theses.ulaval.ca Internet Source	1%
4	ir.lib.uwo.ca Internet Source	1%
5	Rahbar-Ranji, A.. "Dynamic Magnification Factor in a Box-Shape Steel Girder", Journal of The Institution of Engineers (India) Series C, 2014. Publication	<1%
6	ijaiem.org Internet Source	<1%
7	Submitted to University of the West Indies Student Paper	<1%
	Submitted to Thapar University, Patiala	